Bull. Min. Res. Exp. (2026) 179: 81-106

Bulletin of the Mineral Research and Exploration

http://bulletin.mta.gov.tr

Element enrichments and modes of occurrence in the feed coals and coal ashes of the Türkiye thermal power plants

Emine CİCİOĞLU SÜTCÜ[a*], Tolga GÖRMÜŞ[a], Mert Yener BAYRAK[a] and Semra Meltem KADINKIZ[a]

[a] *General Directorate of Mineral Research and Exploration, Mineral Analysis and Technology Department 06530, Ankara, Türkiye.*

Research Article

Keywords:
Fly Ash, Feed Coal, Trace Element, Element Enrichments.

Received Date: 14.12.2024
Accepted Date: 28.04.2025

ABSTRACT

The trace elements enrichments and modes of occurrence were investigated in the feed coals and coal ashes from the thermal power plants Tunçbilek (Kütahya), Soma-Torku and Soma-Kolin (Manisa), Çan 18 Mart (Çanakkale), Yatağan, Yeniköy, Kemerköy (Muğla), Tufanbeyli (Adana), Çatalağzı (Zonguldak), Çayırhan (Ankara), and Elbistan-B (Kahramanmaraş). The Ni, As, Cr and Th concentrations are higher than the World coal averages in the feed coals of almost all power plants. On the other hand, Ni, Cr, Rb, As, and V in the bottom ashes and Ni, Cr, As, U, B, Li, V, Rb, Cd, and Zn in the fly ashes, are higher than the World coal ash averages. The similar element enrichments were observed in both the bottom and fly ashes related to the element enrichments in the feed coals. Siderophile and chalcophile elements such as Ni, Zn, Pb, and Cd are generally associated with iron oxides, spinels, or metal carbonates in coals and coal ashes. In contrast, lithophile elements such as Li, U, B, Th, Ba, Sr, and V are typically present within carbonates, borates, sulfates, oxides, or organic matter in coals, whereas, in ashes, they are more commonly associated with glass phases, carbonates, and sulfates.

1. Introduction

Coal is a major resource that currently provides 41% of global energy needs. It is used not only for electricity generation, but also as a raw material in several industries, including metallurgy, gasification, cement, activated carbon, and industrial chemicals. Furthermore, in recent years, coal and coal ashes have been considered potential alternative resource for elements such as Ge, Ga, U, V, Se, rare earth elements (REE), Sc, Y, Nb, platinum group elements (PGE), Au, Ag, Re, Al, and Mg. The world economy is largely dependent on some critical elements, both in terms of energy efficiency and in stimulating technological advances recently. The critical elements have become rarer and more expensive due to the depletion of ore resources produced by traditional methods and the rapid growth of demand for the elements due to their wide usage areas. Since the supply of many critical elements is related to limited sources, the search for alternative sources such as coal and coal combustion products in their supply has gained great global importance. Depending on various factors such as coal characteristics and combustion method, generally 10-15% of hard coal and 20-50% of lignite remain as ash after combustion. The amount of fly ash emerging in the world today is around 600 million tons per year. The coal-fired power plants in Türkiye release approximately 20 million tons of ash per year, with about 75-80% being fly ash and 20-25% being bottom

Citation Info: Cicioğlu Sütcü, E., Görmüş, T., Bayrak, M. Y., Kadınkız, S., M. 2026. Element enrichments and modes of occurrence in the feed coals and coal ashes of the Türkiye thermal power plants. Bulletin of the Mineral Research and Exploration 179, 81-106. https://doi.org/10.19111/bulletinofmre.1793942

*Corresponding author: Emine CİCİOĞLU SÜTCÜ, sutcuemine@gmail.com

ash. Recently, some studies have been carried out to explore the possibility of extracting rare earth and other metallic elements from coal and coal ashes in the World, especially in America, China, and Russia. Some of these studies have yielded promising results. Previous studies have shown that concentrations of these elements in some coals and coal combustion products are close to or much higher than the grades of conventional ores (Hower et al., 1999, 2016; Mardon and Hower, 2004; Seredin et al., 2006; Zhuang et al., 2006; Dai et al., 2008, 2011, 2015, 2016, 2018; Seredin and Finkelman, 2008; Du et al., 2009; Franus et al., 2015; Taggart et al., 2016; Lin et al., 2017). Ge, U, V, and Se elements have been recovered from coal and used industrially for a long time. Additionally, Au and Ag elements were obtained from Wyoming and Utah coals (USA) during the late 19th and early 20th centuries. After World War II, coal became the main source of U for the USA and Russia. In the early 1960s, small amounts of Ge were recovered from coal in the Czech Republic, England, Japan, and Russia (Dai et al., 2016). Germanium has been still produced from such coals in Uzbekistan, Russia, and China (Seredin et al., 2006; Höll et al., 2007). There are also many studies in Türkiye about the coal characteristics, element concentrations, and hazardous air pollutants in coal and coal ashes (Karayiğit et al., 2000*a*, Kalyoncu et al., 2021; Shanmugam, 2024). The studies fundamentally focused on the environmental effects of elements. On the other hand, the concentration, distribution, and origin of the elements such as As, Sb, Ba, Ni, Cr, that have high concentrations in some Turkish coals were reported by Querol et al. (1997), Karayiğit et al. (2000*a,* 2000*b,* 2001, 2019), Cicioğlu (2001), Karayiğit and Çelik (2003), Palmer et al. (2004), Vassilev et al. (2005), Gürdal (2008), Sütcü and Karayiğit (2015), Baba et al. (2016), Sütcü (2021), Sütcü et al. (2021), Aykaç et al. (2023), Çöteli et al. (2025). Karayiğit et al. (2000*a*) studied feed coals of the Çayırhan, Seyitömer, Tunçbilek, Orhaneli, Soma, Yatağan, Yeniköy, Elbistan, Kangal, and Çatalağzı thermal power plants for the hazardous air pollutants (HAP). Previous studies have shown that Turkish coals are enriched in many elements. It has been supposed that the ashes from power plants derived from the element enriched coals, could be used as an alternative source of these elements. This study examined the elemental compositions of feed coals, bottom ashes, and fly ashes from selected power plants in Türkiye to evaluate the potential of coal and coal ashes as a source of elements.

2. Materials and Methods

The coal-fired power plants that used indigenous coals and fed from the basins with large coal reserves were selected for the sampling. The feed coal, bottom and fly ash samples were taken from the Kütahya-Tunçbilek, Manisa-Soma-Torku, Manisa-Soma-Kolin, Çanakkale-Çan 18 Mart, Muğla-Yatağan, Muğla-Yeniköy, Muğla-Kemerköy, Adana-Tufanbeyli, Zonguldak-Çatalağzı, Ankara-Çayırhan and Kahramanmaraş-Elbistan B Power Plants (Figure 1). The detailed information about the power plants is listed in Table 1.

In this study, thermal power plants supplying coal from certain coalfields have been selected to ensure uniformity in coal and ash properties. Samples were collected from the feed coal, fly ash, and bottom ash of the thermal power plant at each work shift over three days, and representative feed coal, fly ash, and bottom ash samples, with each weighing between 25 to 50 kg, were prepared from these collected samples. These procedures were conducted for each power plant. Nevertheless, the feed coal and coal ashes have been collected separately from the units of the Soma-Torku (units 1-4 and 5-6) and Tunçbilek (units A and B) thermal power plants. In total, thirteen feed coals, thirteen fly ashes, and twelve bottom ashes (except Çayırhan Thermal Power Plant) were sampled. The feed coal and bottom ash samples were crushed and ground to 1 mm grain size. The fly ash samples were reduced to a weight of approximately 5-6 kg with a divider. Furthermore, the fly ashes were separated into five fractions by passing them through sieve meshes with sizes of 106, 75, 53, and 38 µm to determine the grain size distribution of fly ashes. The fractions were classified as +106, -106 +75, -75 +53, -53 +38 and -38 µm (Table 2). As seen in Table 2 and Figure 2, the particles less than 38 µm generally represent more than 50 percent of the fly ashes. Only the Soma-Torku and Elbistan-B samples have lower values for the -38 fraction, on the other hand these samples have higher values for the +106 fraction which can be related to

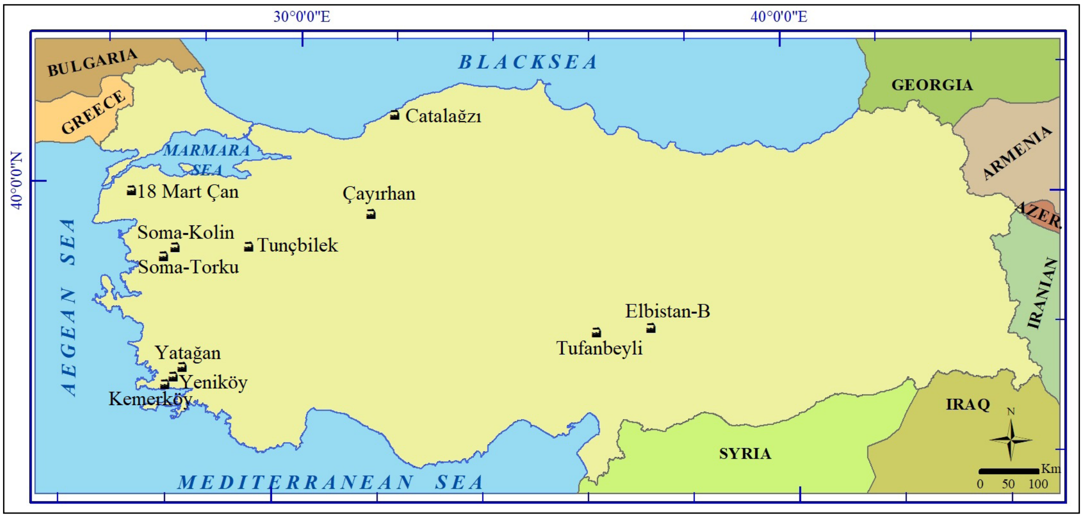

Figure 1- Distribution of the thermal power plants sampled.

Table 1- The properties of studied thermal power plants (Palmer et al., 2004; Tamzok, 2017; Enerji Atlası, 2024).

Thermal Power Plants	Power Capacity (MW)	Ash production (tones/year)	Coal Supply	Coal type	Depositional Environment of Coals	Age (Ma)	Combustion technology
Soma-Torku	900	2.373.439	Işıklar, Eynez, N-Kısrakdere	Sub-bituminous	Limnic, continental with volcanic intercalations	Miocene	Pulverise
Soma-Kolin	510	-	Deniş1B Deniş1C	Sub-bituminous		Pliocene	Circulated Fluidized-bed
Kütahya-Tunçbilek		591.854	Tunçbilek	Sub-bituminous		Miocene	Pulverise
Çanakkale-Çan 18 Mart	320	453.440	Çan	Sub-bituminous			Circulated Fluidized-bed
Ankara-Çayırhan	620	-	Çayırhan	Lignite			Pulverise
Muğla-Yatağan	630	1.320.570	Yatağan	Lignite	Limnic	Miocene	Pulverise
Muğla-Yeniköy	420	713.847	Sekköy, İkizköy, Akbelen, Karacahisar	Lignite			Pulverise
Muğla-Kemerköy	630	1.585.195	Hüsamlar, Çakıralan-Belentepe	Lignite			Pulverise
Adana-Tufanbeyli	450	-	Tufanbeyli	Lignite	Fluvial, Limnic, continental with volcanic intercalations	Miyosen Pliocene	Circulated Fluidized-bed
K.Maraş-Elbistan B	1440	6.141.137	Afşin-Çoğulhan-Çöllolar	Lignite			Pulverise
Zonguldak-Çatalağzı	315	803.703	Çatalağzı and Zonguldak coal washer wastes	Bituminous coal washer wastes	-	-	Pulverise

the burning yield of the thermal power plants. When there is no complete combustion in the boiler, some combustible materials cannot burn and remain in the coal ashes. On the contrary, the majority of the Kolin, Çan, and Tufanbeyli samples were composed of the -38 fraction. The co-feature of these samples is the burning products of CFB technology which has a high burning yield.

The inductively coupled plasma atomic emission spectroscopy (ICP-OES), inductively coupled plasma-mass spectrometry (ICP-MS), X-ray fluorescence (XRF), X-ray diffraction (XRD), and scanning electron microscopy (SEM) analyses were carried out at the General Directorate of Mineral Research and Exploration (MTA) laboratories in Ankara, Türkiye. The samples were prepared according to the American Society for Testing and Materials (ASTM) D2013/D2013M-18 Standard for the analysis.

The United States Environmental Protection Agency (EPA) Method 5050 and EPA 7473 methods

Table 2- The percentages of grain size distributions in the fly ash samples.

	TA-FA	TB-FA	SK-FA	S56-FA	S14-FA	ÇAN-FA	ELB-FA	ÇAY-FA	TUF-FA	YAT-FA	KEM-FA	YEN-FA	ÇAT-FA
Grain size interval (μm)	Weight %												
+106	11.4	24.1	1.5	19.7	40.7	5.8	28.9	15.2	0.7	16.6	17.3	19.9	9.8
-106+75	9.5	8.7	1.0	11.5	11.8	10.1	11.2	7.5	4.2	10.5	7.9	8.9	6.0
-75+53	9.7	7.3	8.3	11.9	10.3	15.3	11.6	7.14	7.0	7.3	7.9	8.3	6.1
-53+38	11.3	7.7	15.3	11.7	8.0	12.6	9.7	7.8	15.5	7.4	9.4	8.5	7.4
-38	58.2	52.2	74.0	45.2	29.2	56.2	38.6	62.4	72.7	58.2	57.5	54.4	70.6

TA: Tunçbilek A unit, TB: Tunçbilek B unit, S14: Soma-Torku 1-4 unit, S56: Soma-Torku 5-6 unit, K: Soma-Kolin, Çan: Çan 18 Mart, Elb: Elbistan B, TUF: Tufanbeyli, ÇAY: Çayırhan, YAT: Yatağan, KEM: Kemerköy, YEN: Yeniköy, ÇAT: Çatalağzı.

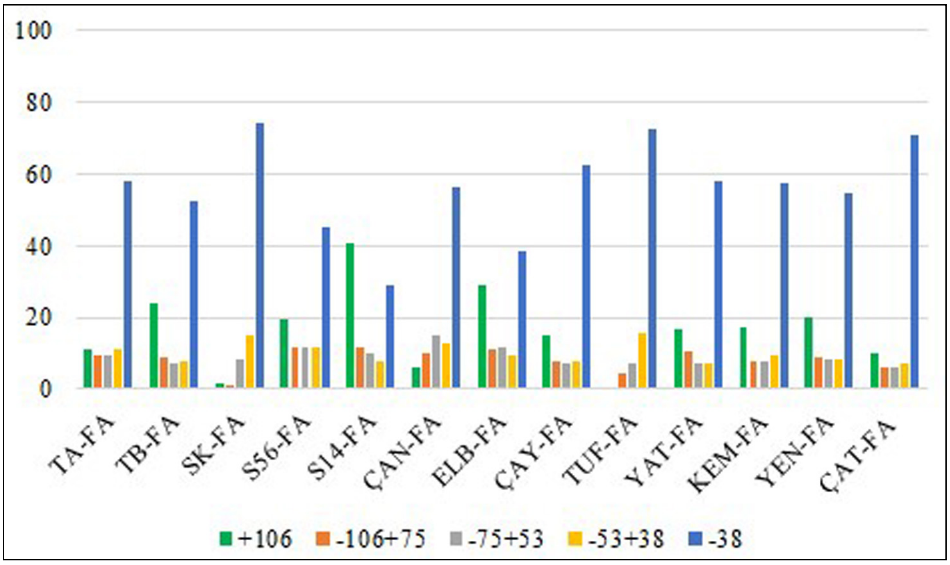

Figure 2- The grain size distribution of the fly ash samples.

were used to determine the total chlorine and mercury content of the samples. The XRD diffraction analysis was carried out using Panalytical X'Pert Powder X-ray diffractometer (Cuα radiation at 40 kV. 30 mA current and 2θ=4 to 70). The major oxides were determined by XRF spectrometry (Thermo-ARL). The powdered samples were held at 815 °C about four hours then they were mixed with cellulose and pressed in 32 mm diameter stainless mold to make pellets for the XRF analysis. The trace element analyses were conducted on Agilent ICP-OES instrument. The samples were digested in perchloric acid ($HClO_4$), nitric acid (HNO_3), and hydrochloric acid (HCl) before the analyses. The Tufanbeyli and Kolin fly ashes and Tunçbilek feed coal were analyzed in FEI Quanta 400 MK2 SEM, EDAX Genesis XM4i energy dispersive scanning (EDS) scanning electron microscope. The surfaces of the fly ash samples were covered with Au-Pd and the feed coal with carbon before the analysis.

3. Results and Discussions

3.1. Mineralogy

The mineral compositions of the feed coals are listed in Table 3. Quartz, K-feldspar, pyrite, and clay minerals are present in all feed coals. Although, the clay minerals show differences in the feed coals, kaolinite and illite are common clay minerals. Vermiculite and smectite were detected in some of the coals. Although not present in all samples, calcite, dolomite, and mica are also common minerals. Some samples contain plagioclase, goethite, sphalerite, apatite, gypsum, Fe-oxides, Zn-spinels (Zn-Cr, Zn-Ga),

Table 3- Mineral composition of the feed coals.

	Silicates										Carbonates				Oxides				Sulfates	Sulfides		Phosph.
	Quartz	Cristobalite	Kaolinite	Vermiculite	Illite	Smectite	Plagioclase	K-Feldspar	Mica Min.	Zeolite Min.	Calcite	Dolomite	Aragonite	Siderite	Magnesioferrite	Goethite	Zn-Spinel	Cd-Zn-Ni-ferrite	Gypsum	Pyrite	Sphalerite	Apatite
TA-FC	+	+	+	+		+		+		+		+		+	+	+	+	+		+		+
TB-FC	+		+	+				+		+		+		+	+	+	+	+		+		+
S14-FC	+		+	+	+			+	+	+	+	+			+	+	+	+	+	+		
S56-FC	+		+	+	+			+	+	+	+				+	+	+	+	+	+		
K-FC	+		+	+	+			+	+	+	+				+	+	+	+	+	+		
ÇAN-FC	+	+	+		+		+	+	+	+	+	+							+	+	+	
ELB-FC	+		+		+			+		+	+	+	+						+	+		+
TUF-FC	+		+		+			+	+	+	+	+	+		+				+	+	+	+
ÇAY-FC	+	+	+	+		+	+	+	+	+	+	+			+				+	+		
YAT-FC	+		+	+	+			+	+		+				+			+	+	+	+	+
KEM-FC	+		+	+	+			+	+		+				+			+	+	+	+	+
YEN-FC	+		+	+	+			+	+		+	+			+			+	+	+	+	+
ÇAT-FC	+			+	+	+	+	+			+	+							+	+	+	+

and zeolite minerals. The feed coals from the basins having volcanic inputs are rich in K-feldspar and zeolite group minerals, while coals from basins with carbonate and ophiolitic basement rocks contain abundant carbonate and phosphate minerals, Fe-oxides, and Zn-Cr-Ni-spinels. In addition, minor amounts of baryte, Fe-Mg-oxides, Fe-Ti-oxides, Fe-Ni-Cr oxides, monazite, zircon, galena, chromite minerals were observed in Tunçbilek feed coal during the SEM analysis. Magnesioferrite, Cd-Zn-Ni ferrite were also detected with the XRD analyses of some feed coals (Table 3).

The bottom ash and fly ash samples contain similar mineral compositions in the studied samples (Table 4). The mineral composition of coal ashes is primarily influenced by the type of coal, boiler, combustion temperature, and the method of ash storage. The coal ashes consist of glassy (non-crystalline) and crystalline components, depending on their types. These constituents can be classified into three groups: (a) the primary minerals inherited from coal such as some stable silicates, oxides, sulfates, phosphates, carbonates, and others (b) the secondary phases formed during combustion such as various silicates, oxides, sulfates, carbonates, sulfides, glass, and char (c) tertiary phases crystallizing during transport and storage in a disposal site such as portlandite, brucite, gypsum, Fe-sulfate, calcite, dolomite, Fe and Al hydroxides, and amorphous material (Vassilev and Vassileva, 1996*a*; Pedziwiatr et al., 2021).

In the studied ash samples, the main components are represented by silicates, sulfates, carbonates, oxides and glassy phases (Figure 3). Quartz and anorthite from the silicate group were detected in almost all ashes. Anorthite can be both primary and secondary in the samples. The presence of anorthite in the feed coals supports primary origin. Some feldspars, especially basic plagioclases, may form through solid-phase reactions between aluminosilicates and liberated Ca, K and Na oxides during burning (Vassilev and Vassileva, 1996*b*). Anorthite can also form from the melts of Ca-rich ashes. Consequently, anorthite is more likely to be found in the Ca-rich class C fly ashes than in class F fly ashes (Hower, 2012). In the studied ashes, most of the glass phases having anorthite chemistry were commonly observed during the SEM analysis (Figure 4a).

Table 4- Mineral composition of the bottom and fly ashes.

	Silicates									Carbonates			Oxides							Sulfates			Sulfides	Phosph.
	Quartz	Cristobalite	Plagioclase	Mullite	Melilite	Clay Min.	Chlorite	Zeolites	Calcite	Dolomite	Magnesite	Siderite	Lime	Portlandite	Periclase	Manyetite	Spinel	Hematite	Magnesioferrite	Anhydride	Gypsum	Etringite	Sphalerite	Apatite
TA-BA	+		+	+		+		+	+	+						+		+	+		+			+
TB-BA	+		+	+		+		+	+	+						+	+	+	+					+
S14-BA	+		+						+	+						+			+		+			
S56-BA	+		+			+	+		+	+						+			+					
K-BA	+		+						+	+				+			+		+	+	+			
ÇAN-BA	+								+	+			+					+		+				
ELB-BA	+		+			+			+															
TUF-BA	+		+		+				+			+	+					+	+	+			+	+
YAT-BA	+		+	+	+			+	+				+			+	+	+	+	+				+
KEM-BA	+		+			+			+										+	+		+		
YEN-BA	+		+		+	+			+										+	+				
ÇAT-BA	+			+		+			+					+			+	+			+			
TA-FA	+		+	+					+					+		+		+	+	+				
TB-FA	+		+	+					+					+		+		+	+	+				
S14-FA	+		+						+		+		+	+				+	+	+				
S56-FA	+	+	+						+		+		+	+				+	+	+				
K-FA	+		+						+		+		+	+				+	+	+				
ÇAN-FA	+	+	+						+				+	+				+		+				
ELB-FA	+		+						+				+	+				+		+				
TUF-FA	+		+		+						+			+		+		+	+	+		+	+	
ÇAY-FA	+		+					+					+	+	+	+		+	+	+				
YAT-FA	+		+	+	+			+	+				+	+		+	+	+	+	+				+
KEM-FA	+		+		+								+	+				+	+	+				
YEN-FA	+		+		+								+	+				+	+	+				
ÇAT-FA	+		+	+					+				+	+		+		+			+			

Mullite is a secondary mineral in coal ashes, generated mainly due to the decomposition and transformation of clay minerals, and to a lesser degree mica, feldspars and other aluminosilicates, at temperatures commonly above 1000 °C (Vassilev and Vassileva, 1996*b*). The boiler temperature is important for the formation of mullite therefore it is not observed in ashes from fluidized bed combustion technology. The clay minerals such as kaolinite, illite, vermiculite, and smectite in the feed coals, generally melt at high temperatures and pass dominantly into the glass phases or mullite during combustion. Mullite has been identified in some bottom and fly ash samples (Figure 4a). The melilite series is a group of sorosilicate minerals can be found in blast-furnace slags. In the samples, melilite was detected in the Tufanbeyli, Yatağan, Kemerköy and Yeniköy ashes (Figure 4c). Calcite and dolomite are observed mainly in the bottom ashes of Tunçbilek, Soma-Torku, Soma-Kolin, and Çan power plants whereas the other bottom ashes contain only calcite. Calcite is the main carbonate mineral found in fly ashes. It can be present in ashes as a primary mineral inherited from coal, even though relatively high temperatures (>850 °C) in boilers

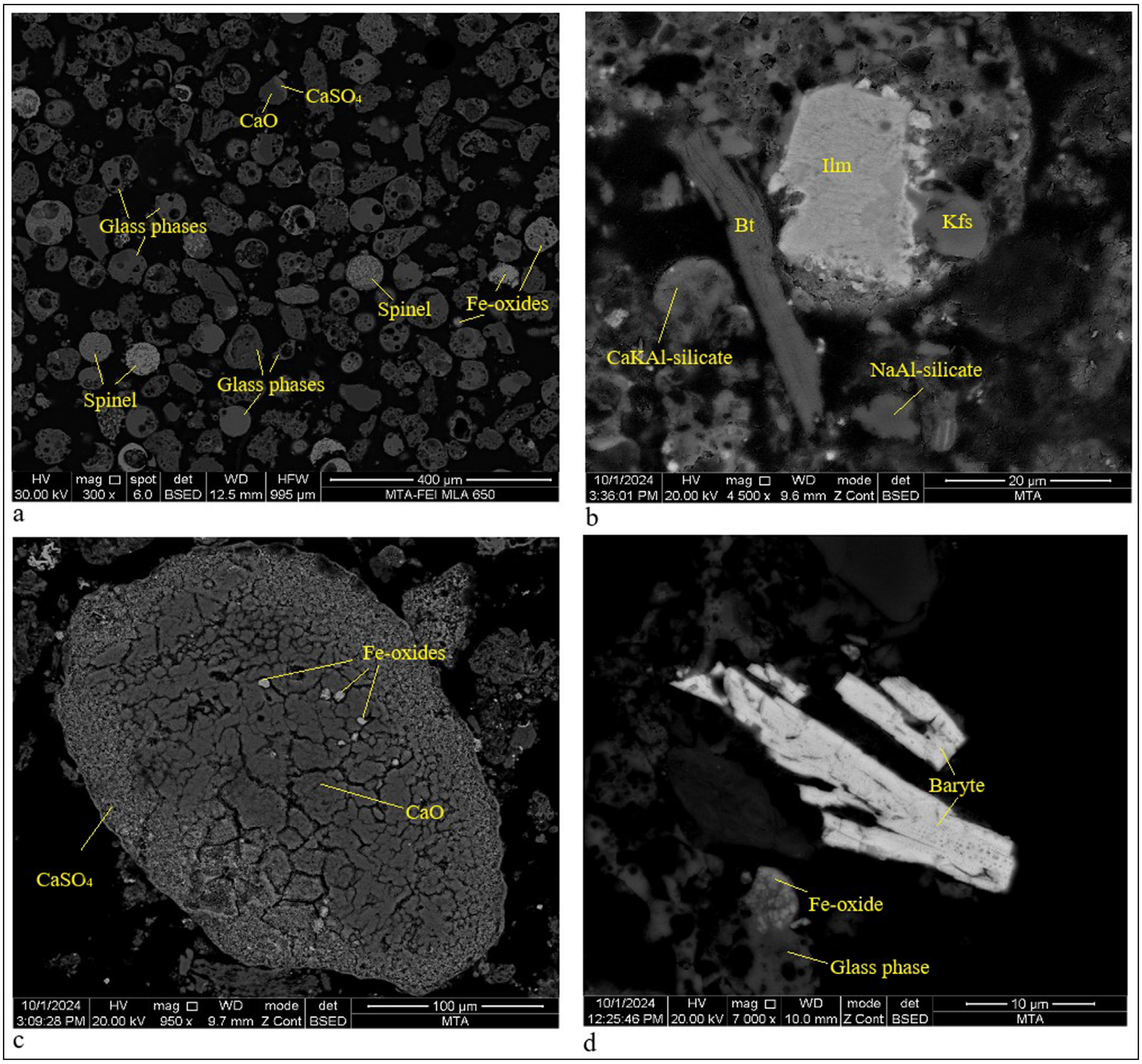

Figure 3- SEM images of the Tunçbilek, Tufanbeyli and Kolin fly ashes, a) Backscatter view of Tunçbilek fly ash, b) Mg-Mn bearing ilmenite, biotite, Ca-Fe bearing NaAl-silicate, Fe-Na-Ca bearing K-feldspar, c) CaO alternation into $CaSO_4$ and d) Baryte, Fe-oxide and glass phase. (Ilm: Ilmenite; Bt: Biotite; Kfs: K-feldspar)

should degrade this mineral to lime (Pedziwiatr et al., 2021). The presence of calcite in ashes from thermal power plants can be related to the unequal heating of primary calcite in boilers and the reaction of lime with atmospheric CO_2 (Demir et al., 2001). The oxides in the ashes are represented by lime, portlandite, hematite, magnetite, periclase, and spinel forms. Lime, portlandite and hematite are commonly observed in the fly ashes (Figure 3). Magnetite, spinel, and periclase are observed in some bottom and fly ashes. Pedziwiatr et al. (2021) highlighted that the ashes from boilers using fluidized bed combustion contain a high level of lime, contrasting with low lime content found in ashes from conventional pulverized coal combustion technology. This difference is associated with the lower boiler temperatures, reaching up to 820 °C, and the addition of $CaCO_3$ (or other calcium-rich materials) to the coal in this type of technology (Perna et al., 2018). Lime (CaO) can also transform into portlandite and last calcite during ash storage (Vassilev and Vassileva, 2007). SO_2 released from coal combustion reacts with lime (CaO), calcite ($CaCO_3$), or sometimes $Mg(OH)_2$. The reaction produces calcium or magnesium sulfite ($CaSO_3$), which further

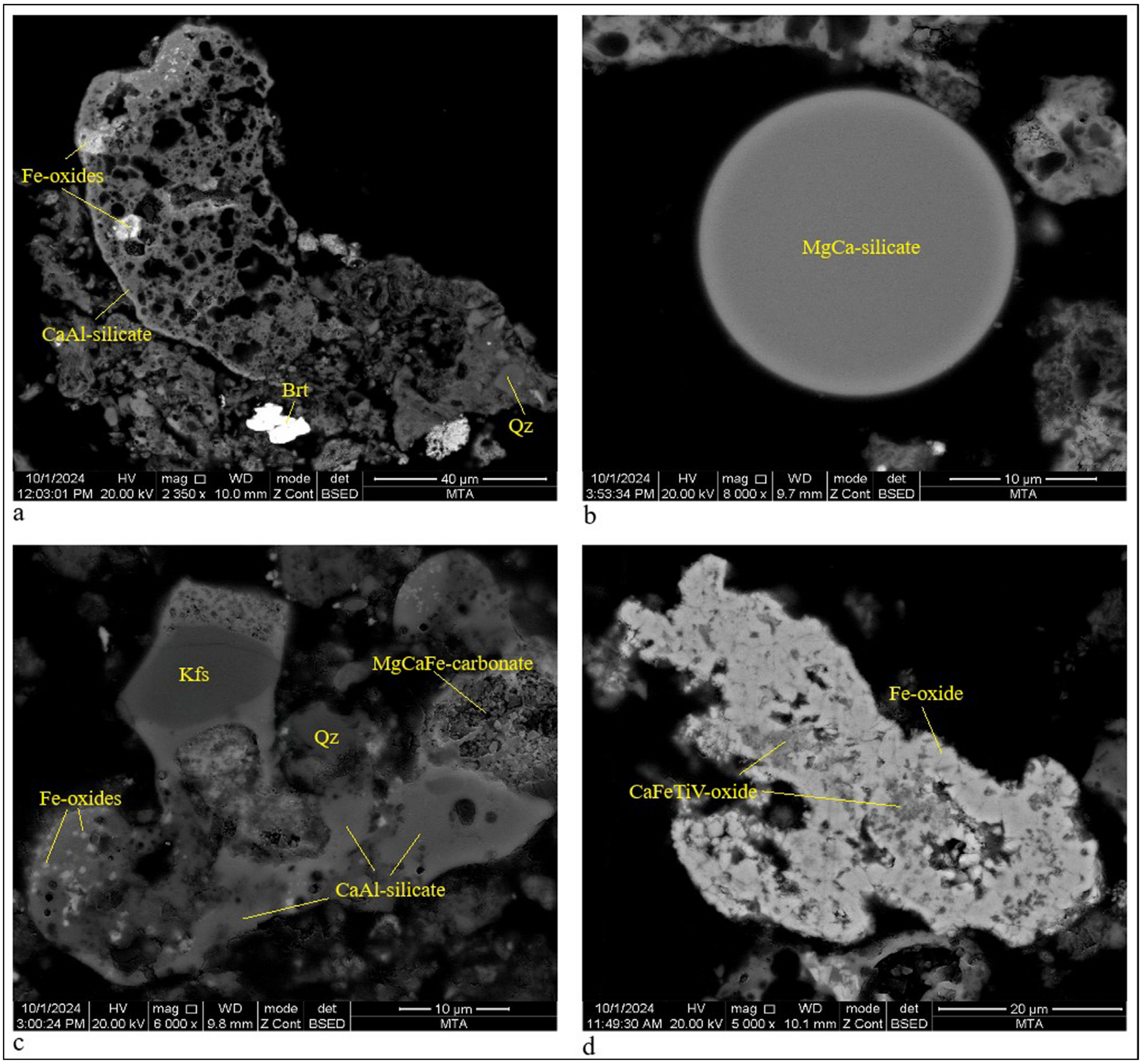

Figure 4- SEM images of the Tufanbeyli and Kolin fly ashes, a) Mullite, glassy phase with anorthite chemisrty, baryte, Fe-oxides, and quartz, b) Glassy sphere (Ca-Mg silicate with minör amount Al and Fe), c) K-feldspar, Mg-Ti-Fe-S bearing melilite (Ca-Al silicate), quartz, and Fe-oxides and d) Fe-oxide and Ca-Ti-V bearing Fe-oxide (Brt: Baryte; Kfs: K-feldspar; Qz: Quartz).

oxidizes to form $CaSO_4 \cdot 2H_2O$ (Figure 3c). Anhydrite and gypsum are common minerals that occur at the end of this reaction. If gypsum occurs as a primary mineral in coals, low-temperature combustion allows gypsum to undergo dehydration to bassanite and anhydrite (Vassilev and Vassileva, 1996*b*). Hence, gypsum is generally not observed in fly ash samples. As it was stated before portlandite is the tertiary phase mineral crystallizing during transport and storage in a disposal site. Therefore, anhydrite and portlandite are present in all samples and gypsum is observed generally in the bottom ashes. Ettringite, the other sulfate mineral, was detected only in the Kemerköy and Tufanbeyli ashes. High-calcium fly ashes contain appreciable amounts of soluble calcium, aluminum, and sulfur-bearing minerals, and calcium aluminate glass (Figure 4) that are favorable for ettringite formation (Tishmack et al., 1999). The sulfide minerals such as pyrite and sphalerite are converted into Fe- and Zn-oxides like hematite, magnetite, and spinels. Pyrite generally transforms into pyrrhotite at 250-850 °C and afterward into hematite at >850 °C during the coal combustion (Demir et al., 2001). Vasilev and Vasileva (1996*b*) indicated that the coarse-grained fly and bottom ashes are normally more abundant in magnetite than fine-grained fly ash enriched in hematite. This case demonstrates a relatively higher oxidizing condition during the formation of finer fly ash. In the studied ash samples hematite are present all fly ashes and some bottom ashes whereas magnetite is only observed in the Tunçbilek, Soma-Torku, Tufanbeyli, Yatağan, Çayırhan and Çatalağzı ashes. Spinel can be primary and secondary, when its formation is a result of probable solid-phase reaction between Mg, Al and Fe oxides, or recrystallization of clay and mica minerals (Vassilev and Vassileva, 1996*b*).

Sphalerite is observed only in the bottom and fly ashes of Tufanbeyli. SEM analysis of Tufanbeyli fly ash revealed the presence of Zn-carbonates formed from the oxidation of sphalerite minerals (Figure 5c). These alternations were observed around the calcite minerals. The Cd-Ni-Zn-ferrite and Zn-spinels were detected on the XRD spectra of the samples. Furthermore, some accessory minerals and phases such as baryte, monazite, ilmenite, zirconium, rutile, Fe-Mn oxides, and Fe-Ni-Cr-oxides were identified during the SEM analysis (Figure 4a, 4c, 4d, and Figure 5).

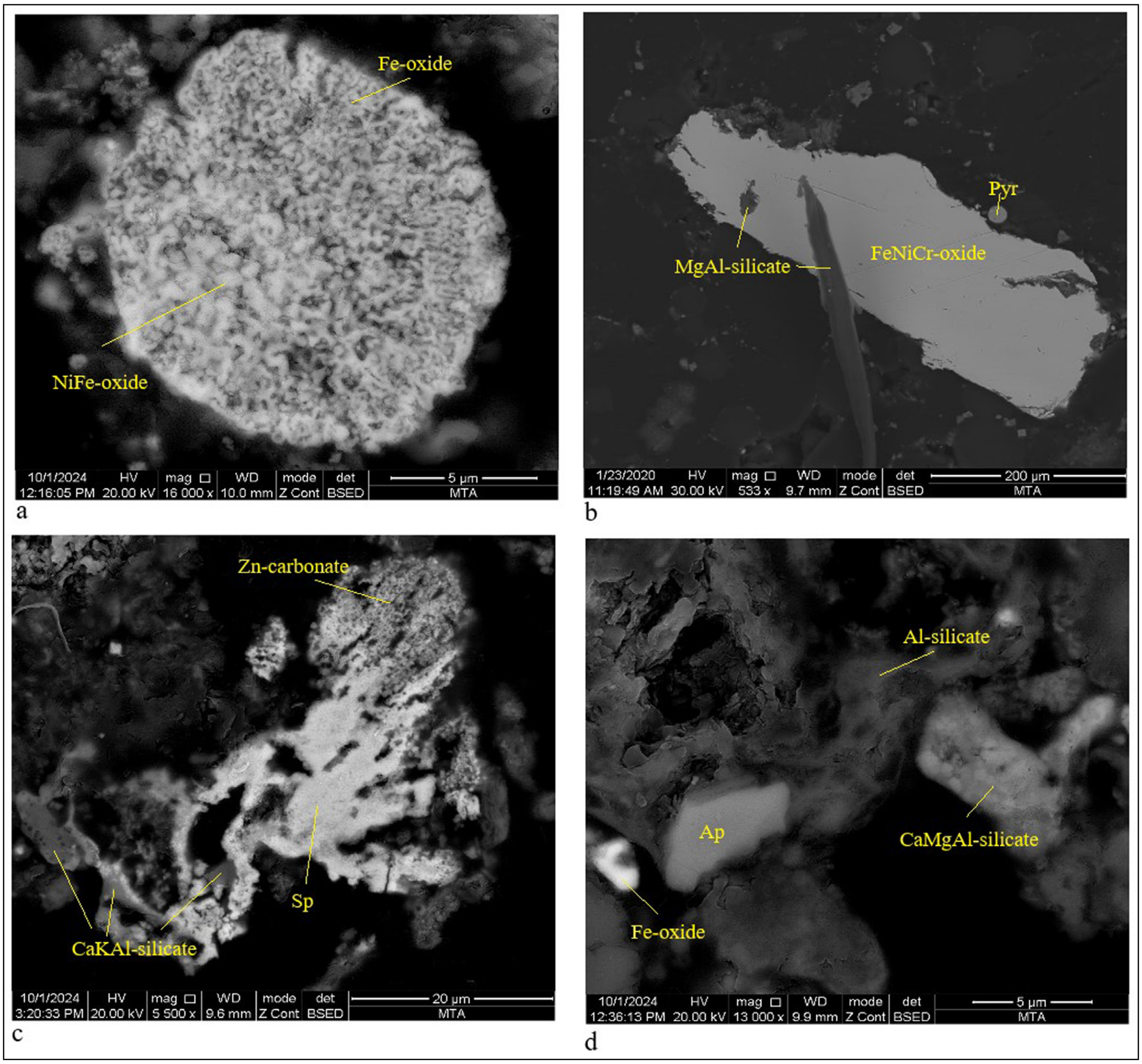

Figure 5- SEM images of the feed coals and fly ashes, a) Ni bearing Fe-oxides in the Kolin fly ash, b) MgAl-silicate and Ni-Cr-Fe-oxide in the Tunçbilek coal, c) Partially oxidized sphalerite (Sp), Zn-carbonate, and Fe-Zn bearing CaKAl-silicate in the Tufanbeyli fly ash and d) F-apatite (Ap), Fe-V-Ti bearing CaMgAl-carbonate and Fe-Ca-K-Ti-Mg bearing glassy phase with Al-silicate chemistry in the Kolin fly ash (Ap: Apatite; Pyr: Pyrite; Sp: Sphalerite).

3.2. Major Oxides

3.2.1. Feed Coals

The major oxide distributions of the feed coals are listed in Table 5. The most abundant major oxides are Al_2O_3 and SiO_2, followed by CaO and SO_3. The concentrations of Fe_2O_3 are slightly higher in the Tunçbilek, Çan, Elbistan, and Çatalağzı samples, while MgO levels are higher in the Tunçbilek samples compared to the others.

The clay minerals such as kaolinite, illite, smectite, mica minerals, K-feldspar and anorthite can be the sources of Al_2O_3, K_2O and SiO_2 in the feed coals. In addition, the SiO_2 concentration can also be related to quartz, cristobalite, vermiculite, mica, and zeolite minerals. Vassilev and Vassileva (1996*a*) indicated that the volcanic glass in coals predominantly has an aluminosilicate or titanium-rich composition, with minor Ca, Fe, Mg, K, Na, P, S, and Cl contents. In Türkiye, many coal basins contain volcanic inputs such as in the Soma, Tunçbilek, Yatağan, Çan, and Çayırhan coalfields. The mineral compositions and major oxide concentrations of these feed coals reflect the effect of volcanic inputs. CaO and P_2O_5 can be mainly related to calcite, apatite, and gypsum minerals. The fossil fragments in the Elbistan coals contain a high amount of Ca and a trace amount of Fe, Mg, Sr, and Mn (Sütcü and Karayiğit, 2015). Vassilev et al. (2005) also indicated that feed coal and fly ash from the Soma power plant contain siderite and ankerite [$Ca(Fe,Mg,Mn)(CO_3)_2$] minerals. Sütcü (2021) indicated that the MgO, CaO, Fe_2O_3, and SO_3 concentrations were sourced from mainly dolomite, ankerite, siderite, gypsum, smectite, and pyrite in the feed coals. On the other hand, SO_3 can also be derived from sulfate minerals. Iron oxides, iron carbonates (siderite), and dolomites may serve as additional sources of Fe_2O_3. The Fe-bearing dolomite and Mg-siderite were observed in the Tunçbilek coals (Sütcü et al., 2021). However, Al_2O_3 and MgO can also be related to clay and mica minerals. TiO_2 concentrations can be related mainly to clay minerals, rutile, and ilmenite minerals.

3.2.2. The Bottom Ashes

The major oxide concentrations in the bottom ashes are similar to those in the feed coals (Table 6). Only the CaO concentration is higher than the feed coals. Although the SO_3 concentration is low in the feed coal samples, it shows a significant increase in the bottom ashes from Kolin, Çan, and Tufanbeyli

Table 5- Major oxide concentrations (%) of the feed coal samples (adb: air-dried basis).

Sample No	Ash% 850°C	C % (adb)	Al_2O_3	CaO	Fe_2O_3	K_2O	MgO	MnO	Na_2O	P_2O_5	SO_3	SiO_2	TiO_2
TA-FC	53.7	39.6	11.12	1.07	4.24	0.75	2.47	0.05	0.11	0.11	1.5	29.77	0.43
TB-FC	62.8	32.3	13.18	1.88	4.71	0.94	2.82	0.06	0.13	0.13	2.07	33.76	0.5
S14-FC	56.8	33.9	6.5	16.8	1.8	0.5	1.2	0	0.2	0.1	3.4	14.5	0.3
S56-FC	63.8	27.1	10.2	15.5	1.9	0.5	0.7	<0.1	0.2	0.1	2.7	20.3	0.5
K-FC	57.6	27.5	11.8	8.7	2.2	0.6	0.6	<0.1	0.2	0.2	3.9	21.2	0.7
ÇAN-FC	48.0	39.35	9.3	1.6	4.3	0.2	0.2	0.1	0.3	0.1	1.4	18.1	0.5
ELB-FC	56.4	28.59	9.3	39	5.2	0.5	1.7	<0.1	0.3	0.4	18.4	23.1	0.8
TUF-FC	55.7	30.62	6.1	8.1	2.3	0.5	0.8	<0.1	0.1	0.1	5.5	11.4	0.3
ÇAY-FC	51.0	28.69	3.9	6.4	2.7	0.7	1.8	<0.1	0.6	0.3	6.5	15.8	0.4
YAT-FC	51.3	47.14	3.9	3.4	2.4	0.3	0.8	<0.1	0.1	0	4	7.3	0.2
KEM-FC	53.6	28.9	8.9	14.4	2.4	0.8	1.2	<0.1	0.4	0.1	7.8	14.1	0.3
YEN-FC	50.4	26.97	10	13.7	2	0.8	1.4	<0.1	0.4	0.1	7.1	15.3	0.3
ÇAT-FC	56.0	39,9	13.8	0.7	3.1	2.1	1.1	<0.1	0.2	0.1	0.5	31.2	0.8

Table 6- Major oxide concentration of bottom ash samples.

Sample No	Al_2O_3	CaO	Fe_2O_3	K_2O	MgO	MnO	Na_2O	P_2O_5	SO_3	SiO_2	TiO_2
TA-BA	20.3	3.2	10.2	1.4	5.2	0.2	0.2	0.2	2.0	54.4	0.8
TB-BA	19.7	3.3	10.4	1.6	5.6	0.2	0.2	0.2	1.1	55.6	0.8
S14-BA	9.50	46.9	4.2	0.8	3.3	0.1	0.3	0.2	5.8	26.0	0.6
S56-BA	16.2	29.8	4.5	1.0	1.5	0.1	0.4	0.2	6.2	36.4	0.9
K-BA	20.5	18.7	4.0	1.1	1.1	<0.1	0.3	0.2	12.3	38.4	1.2
ÇAN-BA	19.2	21.8	4.5	0.4	0.8	0.2	0.4	0.2	13.8	37.4	1.1
ELB-BA	13.6	28	7.4	0.8	1.9	0.1	0.4	0.4	7.5	35.4	1.1
TUF-BA	18.4	18.9	5.2	1.0	1.3	<0.1	0.3	0.2	13.2	31.7	1.4
YAT-BA	17.8	17.5	9.2	2.0	2.1	0.1	0.5	0.2	3.5	45.6	1.1
KEM-BA	19.2	25.8	5.7	1.8	2.3	0.1	0.6	0.4	7.1	31.9	0.7
YEN-BA	18.4	30.4	4.9	1.7	2.6	0.1	0.6	0.3	6.7	29.5	0.7
ÇAT-BA	23.8	1.6	6.9	3.9	2.0	0.1	0.9	0.1	0.6	58.1	1.4

power plants. These power plants have circulating fluidized bed (CFB) technology that is a relatively new technology with the ability to achieve lower emission of pollutants. In this technology, sulfur-absorbing chemicals such as limestone and dolomite are added to the coal particles during the fluidization phase to absorb the sulfur pollutants released during the burning process. Therefore, the CaO and SO_3 concentrations in the bottom ashes are higher than those in the feed coals. The sulfur-absorbing chemicals are also used in pulverized type power plants to absorb the sulfur. However, their quantity of usage is lesser than the CFB power plant's. Hence, related to the combustion technology, Kolin, Çan, and Tufanbeyli bottom ashes have higher SO_3 values. The source of SiO_2 and Al_2O_3 can be related to glassy phase and silicate minerals. CaO, P_2O_5, and SO_3 concentrations can be mostly related to calcite, dolomite, anorthite, lime, anhydrite, portlandite, gypsum, and apatite. However, glass spheres with Ca-Mg silicate and Ca-Al-silicate compositions were observed in the Tufanbeyli and Kolin fly ashes (Figure 4a and 4b). Magnetite, hematite, Fe-oxides, and Fe-carbonates are potential sources of Fe_2O_3. MgO was also detected in the carbonates (dolomite, calcite), silicates (anorthite, oligoclase, glassy phase, and mullite) and Fe-oxides and siderite during the SEM analysis (Figure 4).

The bottom ash samples were classified by using ASTM C 618-22 and Turkish Standards Institution (TS-EN) 197-1 standards. Since the SiO_2+Al_2O_3+Fe_2O_3 content in the bottom ashes is over 70% and the CaO value is less than 10%, the Tunçbilek and Çatalağzı bottom ashes are classified as F class (low lime). Although, the Soma 5-6 unit, Kolin, Çan, Elbistan, Kemerköy, and Yeniköy bottom ashes meet class C criteria with the SiO_2+Al_2O_3+Fe_2O_3 values exceeding 50% and the CaO values above 10%, but the SO_3 values are not in the limits (max 5%) of ASTM C 618-22. Only the Yatağan bottom ash meets all class C criteria of the ASTM C 618-22 Standard. The Soma 1-4 unit bottom ash is classified as "off-specification" ash because it does not meet the requirements for either Class C or Class F criteria in ASTM C 618-22. On the other hand, the bottom ashes from Soma, Kolin, Çan, Tufanbeyli, Elbistan, Yatağan, Kemerköy, and Yeniköy power plants, can be classified as Class W ashes under the TS-EN 197-1 standard, as they have CaO value being over 10% and Al_2O_3+SiO_2 values being over 25%. The Tunçbilek and Çatalağzı ashes meet the Class V criteria of TS-EN 197-1 standard.

3.2.3. The Fly Ashes

The major oxide concentrations of the fly ash samples are listed in Table 7. CaO and SiO_2 are the

Table 7- Major oxide concentration of fly ash samples.

Sample No	Al_2O_3	CaO	Fe_2O_3	K_2O	MgO	MnO	Na_2O	P_2O_5	SO_3	SiO_2	TiO_2
TA-FA	22.2	2.2	8.9	1.5	4.2	0.2	0.2	0.2	0.9	57.0	1.0
TB-FA	21.6	2.5	8.5	1.8	4.5	0.2	0.2	0.2	1.1	56.8	0.9
S14-FA	13.8	37.6	4.3	1.1	2.2	0.1	0.5	0.2	7.0	32.1	0.9
S56-FA	20.2	26.7	3.8	1.2	1.3	<0.1	0.4	0.2	3.8	41.0	1.1
K-FA	18.4	19.2	4.9	0.9	1.2	<0.1	0.3	0.2	12.5	31.4	1.4
ÇAN-FA	20.0	20.6	9.4	0.3	0.5	0.1	0.6	0.2	10.9	33.9	1.1
ELB-FA	11.2	37.9	5.9	0.6	1.8	<0.1	0.4	0.4	12.8	27.9	0.9
TUF-FA	20.0	20.6	9.4	0.3	0.5	0.1	0.6	0.2	10.9	33.9	1.1
ÇAY-FA	20.0	20.6	9.4	0.3	0.5	<0.1	0.6	0.2	10.9	33.9	1.1
YAT-FA	17.6	17.6	9.1	2.0	2.2	0.1	0.6	0.2	3.4	45.6	1.1
KEM-FA	19.4	25.8	5.9	2.2	2.0	<0.1	0.8	0.3	9.7	32.1	0.8
YEN-FA	20.5	26.2	5.1	2.2	2.5	0.1	0.9	0.3	8.8	32.2	0.8
ÇAT-FA	25.2	1.6	6.3	3.8	2.0	0.1	1.8	0.2	0.9	55.9	1.6

dominant major oxides in the samples followed by Al_2O_3, SO_3, and Fe_2O_3. The SiO_2 and Al_2O_3 contents are similar to those in the bottom ashes. However, the CaO content in the fly ashes is lower than in the bottom ashes, except for the Çatalağzı and Soma5-6 unit samples. The Fe_2O_3 concentration in the Tufanbeyli and Tunçbilek fly ashes is lower than in their bottom ashes. The MgO, K_2O, MnO, Na_2O, P_2O_5 and TiO_2 major oxides do not show significant changes compared to the bottom ashes. The Al_2O_3, K_2O, TiO_2, SiO_2 concentrations can be mainly related to the quartz, plagioclase, K-feldspar, mullite, melilite, clay and zeolite minerals. The glassy phase also has Ca-Al-K-Ti silicate chemistry. During the SEM analysis of the Tufanbeyli and Kolin fly ashes, the glassy spheres and amorphous glassy phases with Al-silicate, Al-Ca-silicate, Al-K-silicate chemistry with trace amounts of Fe, Ti, V, and Mg were commonly observed (Figure 3 and 4). Fe_2O_3 is primarily related to iron oxides. On the other hand, Fe bearing silicate (K-feldspar, clay minerals) and carbonate (dolomite, siderite) minerals were also observed during the SEM analysis. The CaO concentration can be related to the carbonate (dolomite, calcite), silicate (anorthite, melilite), oxide (portlandite, lime), phosphate (apatite), and sulfate (gypsum, anhydrite) minerals. In addition, the glassy phases have also Ca-Al, Ca-K-Al, and Ca-Mg silicate chemistry. Apatite and monazite minerals can be the source of P_2O_5 concentration in the ashes. The fly ash samples were classified by using ASTM C 618-22 and TS-EN 197-1 standards. The Soma-14, Kolin, Çan, Elbistan, Tufanbeyli, Çayırhan, Kemerköy, and Yeniköy bottom ashes meet class C criteria with the SiO_2+Al_2O_3+Fe_2O_3 value being over 50% and the CaO value being over 10%, whereas the SO_3 values are not in the limits (max 5%) of ASTM C 618-22. Only the Yatağan and Soma56 unit bottom ashes meet all class C criteria of the ASTM C 618-22 Standard. The Tunçbilek and Çatalağzı fly ashes can be classified as F class (low lime). According to the TS-EN 197-1 Standard, the Soma, Kolin, Çan, Tufanbeyli, Elbistan, Yatağan, Kemerköy, and Yeniköy bottom ashes can be classified as Class W ashes. On the other hand, Tunçbilek and Çatalağzı ashes meet the Class V criteria of TS-EN 197-1 Standard.

3.3. Trace Elements

3.3.1. Feed Coals

The trace element concentrations in the feed coals are listed in Table 8. The As, B, Ba, Cr, Co, Cu, Ga, Li, Ni, Pb, Rb, Sr, Th, U, V, and Zn concentrations are higher than the World coal averages (Ketris and Yudovich, 2009). The concentration coefficients (CC) of the feed coals were used to evaluate element

Table 8- Trace element concentrations of feed coals (µg/g).

Sample No	Ash 850 °C	As	B	Ba	Cd	Co	Cr	Cu	Ga	Li	Mo	Ni	Pb	Rb	Sb	Se	Sr	Hf	Sc	Th	U	V	Zn	Hg	Cl
TA-FC	53.7	<10	39.2	176	<5	36.9	202	55.9	7.8	14.5	<5	610	19.6	25.7	<10	<5	180	3.4	13.1	24.1	7.3	46.4	64.3	0.3	300
TB-FC	62.8	7.8	46.6	177	<5	44	204	34.9	9.1	23.9	<5	747	25.9	25.9	<10	<5	190	3.2	12.4	27.8	<10	45.3	59.5	0.4	200
S14-FC	56.8	60.2	251	260	<5	3.4	23.8	11	4.5	30	<5	16.5	13	10	<10	6.8	234	0.4	2.9	9.1	16.5	60.7	29	0	0
S56-FC	63.8	36.4	144	403	<5	4.5	38.3	13	7	54	<5	21.7	17	24	<10	<5	221	0.5	4.3	11.5	10.2	75.3	45	0	0
K-FC	57.6	16.1	325	304	<5	6.3	50.7	19	9.8	97	<5	30.6	30	32	<10	<5	358	0.4	5.9	23.1	20.8	155	67	0	0
ELBFC	48.0	21.3	188	565	<5	23	227	51	<5	54.9	14.2	180	28	135	<10	<5	868	8.5	11.2	23	<10	287	119	0.028	200
ÇAN-FC	56.43	604	185	169	<5	9.4	12.4	26	5.6	42.4	<5	11.3	16	30.8	<10	<5	151	4.5	6.1	4.9	<10	60.8	3.4	0.12	600
TUF-FC	55.71	27.9	12	230	<5	4.4	55.9	12	7.5	36.4	4	32.8	12	54.6	<10	<5	137	1.3	4.2	8.4	<10	51.9	203	0.06	200
ÇAY-FC	51.03	52.5	229	117	<5	6.4	82.6	8	4.8	6.1	4.8	102	12	18.9	<10	<5	157	2.2	2.4	10.3	<10	34.9	27.4	0.03	102
YAT-FC	51.3	35.9	39	117	<5	4.8	49.9	21	4.5	13.7	8.8	31.2	8	9	<10	<5	280	0.7	2.9	9.6	<10	40.2	23.4	0.06	200
KEM-FC	53.55	22.5	22	55.2	<5	6.7	47.7	12	3.9	23	5.7	26.2	9	16.6	<5	<5	441	0.1	4.2	2.7	<10	54.1	46.1	0.02	100
YEN-FC	50.38	14.6	34	51.9	<5	6.3	52.9	13	4.3	26.2	3.9	25.2	9	18.6	<5	<5	249	0.1	4.1	2.3	<10	53.4	38.8	0.0338	100
ÇAT-FC	56.0	9.9	13	533	<5	13	50.8	22	9.1	28.8	14.2	34.6	30	117	<10	<5	153	0.7	5.2	14.1	<10	37.7	63.2	0.07	10
WC		7.6	56	150	0.2	4.2	15	15	5.5	10	2.2	9	6.6	10	0.84	1	120	1.2	4.1	3.3	2.9	22	110	0.62	770
WBC		9	47	150	0.2	6	17	16	6	14	2.1	17	9	18	1	1	100	1.2	3.7	3.2	1.9	28	28	0.1	340
Concentration Coeffient (CC)																									
TA-FC		-	0.7	1.2	-	8.8	13.5	3.7	1.4	1.5	-	67.8	3.0	2.6	-	-	1.5	2.8	3.2	7.3	2.5	2.1	0.6	0.5	0.4
TB-FC		1.0	0.8	1.2	-	10.5	13.6	2.3	1.7	2.4	-	83.0	3.9	2.6	-	-	1.6	2.7	3.0	8.4	-	2.1	0.5	0.6	0.3
S14-FC		7.9	4.5	1.7	-	0.8	1.6	0.7	0.8	3.0	-	1.8	2.0	1.0	-	6.8	2.0	0.3	0.7	2.8	5.7	2.8	0.3	0.0	0.0
S56-FC		4.8	2.6	2.7	-	1.1	2.6	0.9	1.3	5.4	-	2.4	2.6	2.4	-	-	1.8	0.4	1.0	3.5	3.5	3.4	0.4	0.0	0.0
K-FC		2.1	5.8	2.0	-	1.5	3.4	1.3	1.8	9.7	-	3.4	4.5	3.2	-	-	3.0	0.3	1.4	7.0	7.2	7.0	0.6	0.0	0.0
ELBFC		2.8	3.4	3.8	-	5.5	15.1	3.4	-	5.5	6.5	20.0	4.2	13.5	-	-	7.2	7.1	2.7	7.0	-	13.0	1.1	0.0	0.3
ÇAN-FC		79.5	3.3	1.1	-	2.2	0.8	1.7	1.0	4.2	-	1.3	2.4	3.1	-	-	1.3	3.8	1.5	1.5	-	2.8	0.0	0.2	0.8
TUF-FC		3.7	0.2	1.5	-	1.0	3.7	0.8	1.4	3.6	1.8	3.6	1.8	5.5	-	-	1.1	1.1	1.0	2.5	-	2.4	1.8	0.1	0.3
ÇAY-FC		6.9	4.1	0.8	-	1.5	5.5	0.5	0.9	0.6	2.2	11.3	1.8	1.9	-	-	1.3	1.8	0.6	3.1	-	1.6	0.2	0.0	0.1
YAT-FC		4.7	0.7	0.8	-	1.1	3.3	1.4	0.8	1.4	4.0	3.5	1.2	0.9	-	-	2.3	0.6	0.7	2.9	-	1.8	0.2	0.1	0.3
KEM-FC		3.0	0.4	0.4	-	1.6	3.2	0.8	0.7	2.3	2.6	2.9	1.4	1.7	-	-	3.7	0.1	1.0	0.8	-	2.5	0.4	0.0	0.1
YEN-FC		1.9	0.6	0.3	-	1.5	3.5	0.9	0.8	2.6	1.8	2.8	1.4	1.9	-	-	2.1	0.1	1.0	0.7	-	2.4	0.4	0.1	0.1
ÇAT-FC		1.1	0.3	3.6	-	2.2	3.0	1.4	1.5	2.1	6.8	2.0	3.4	6.5	-	-	1.5	0.6	1.4	4.4	-	1.3	2.3	0.0	0.7

enrichments in the feed coals. The CC value is defined as the ratio of element concentrations in the coals compared to the averages for World brown coals calculated by Ketris and Yudovich (2009). The Çatalağzı feed coal on the bituminous coal stage was evaluated according to the bituminous coal averages stated by Ketris and Yudovich (2009). Based on the CC values in Table 8, the Tunçbilek feed coals are significantly enriched in Co, Cr, and Ni, enriched in Th, and slightly enriched in Cu, Pb, Rb, Hf, V, Zn, and Hg. The Soma-Kolin feed coal is enriched in Li, Th, U, and V, and slightly enriched in As, Ba, Cr, Ni, Pb, Rb, Sr, and Zn. The Soma 1-4 feed coal is enriched in As, Se, and U and slightly enriched in B, Li, Pb, Sr, Th, and V. Whereas the Soma 5-6 feed coal is enriched in Li and slightly enriched in As, B, Ba, Cr, Pb, Ni, Th, U, V, and Zn. The Elbistan feed coal is significantly enriched in Cr, Ni, Rb, and V, enriched in Co, Li, Mo, Sr, Hf, and Th, and slightly enriched in Sc, Pb, Cu, B, Ba, and As. The Çan feed coal is significantly enriched in As and slightly enriched in B, Co, Li, Pb, Rb, Hf, V, and Cl. The Tufanbeyli feed coal is significantly enriched in Zn, enriched in Rb, and slightly enriched in As, Cr, Li, Ni, Th, and V. The Çayırhan feed coal is significantly enriched in Ni, enriched in As, and slightly enriched in B, Cr, Mo, and Th. The feed coals of the Yatağan, Kemerköy, and Yeniköy power plants have quite similar element enrichment and As, Cr, Mo, Ni, Sr, Th V, Zn Li are generally enriched in the feed coals. The Çatalağzı feed coal is enriched in Mo and Rb, and slightly enriched in Ba, Co, Cr, Li, Ni, Pb, Th, and Zn. Despite the feed coals showing similar element enrichments, some of them are significantly enriched in As, Co, Cr, Ni, and Zn. Palmer et al. (2004) indicated that the average concentrations of Ni, Cr, As, U, Sb, Cs, and V in Turkish coals are higher than in USA lignites and the anomalous enrichments of these elements were linked to the widespread occurrence of ore deposits of Türkiye. The Tethian ophiolite belt is one of the longest in the World and stretches from Spain to the Himalayas (Bozkurt and Mittwede, 2001) that shows its maximum development in Turkey which contains large and numerous deposits of chromite, Ni-rich olivine, and serpentine (Palmer et al., 2004). Although arsenic and other metals are associated with ophiolites (Cina, 1990) and related massive sulfide deposits (Güleç and Erler, 1983), Türkiye is also the site of extensive Sb–As–Tl–Ba deposits. The Neogene volcanic activities in western Anatolia developed contemporaneously with development of NE-trending basins giving rise to formation of thick volcano-sedimentary successions and several mineral deposits (Helvacı, 2019).

In the Western Anatolia and Biga Peninsula which are metallogenic provinces of Türkiye, there are arc magmatism-related skarn, hydrothermal, epithermal, porphyry-type deposits such as Ag-As-Sb-Pb-Zn-Au-Cu mineralizations, baryte and borate deposits in the region (Helvacı, 2019; Sarı et al., 2022). On the other hand, platform carbonate rocks in the southeastern and southern parts of Anatolia host many Pb-Zn, baryte, bauxite, and phosphate deposits. The mineralizations and element anomalies may have influenced the concentration of elements in Turkish coals. Similar element enrichments as noted by Palmer et al. (2004) were observed in the feed coals under study. The SEM analysis and Pearson correlation coefficients were utilized to determine the mineral-element associations in the study (Table 9). The feed coals originate from different coal basins with varying stratigraphic sequences, paleo-depositional environmental conditions, degrees of coalification, and geological ages. It is believed that the associations between minerals and elements may differ based on the characteristics of each coal basin.

As a result, the observed correlations may not accurately represent the true relationships between trace elements and minerals. Hence, the SEM analyses and the geology of the coal basins were considered primarily to interpret the mineral-element relations. The coals from the Tunçbilek and Elbistan basins that are surrounded by ophiolitic rocks are significantly enriched in nickel and chromium. The magnetite minerals derived from ultramafic rocks contain trace amounts of nickel. In environments enrich in Ni ions, Ni can replace Fe and Mg in minerals such as pyrite, siderite, magnetite, and trevorite (Nesse, 2000). Palmer et al. (2004) also stated that the high nickel and the Cr concentration in Turkish coals were linked to the ophiolitic rocks. The positive strong and moderate correlations between Al_2O_3, TiO_2, K_2O, MgO, Co, Cu, Cr, Ni, Mo, Th, and Hg elements also indicate

Table 9- The Pearson correlation coefficients between major oxides and trace elements for the feed coals.

	0.8<r<1 Very strong	0.6<r<0.79 strong	0.4<r<0.59 moderate	0.2<r<0.39 weak
Al_2O_3		Co, Cu, Ni, Sc	Cr, Mo, Th, Hg	Ga, Pb, Cl
CaO	Sr, V		Ba, Cr, Rb, Hf	B, Cu, Li, Mo, Sc
Fe_2O_3	U	Mo, Hf	Cr, Pb, Rb, Sr, Sc, V, Cl	As, Ba, Co, Cu, Ga, Ni, Th, Hg
K_2O			Co, Cr, Cu, Mo, Ni, Sc, Th, Hg	Ga, Pb
MgO			Co, Cr, Ni, Hg	Hf, Sc, Th
Na_2O	U			B
P_2O_5		Sr, Hf, U, V	B, Ba, Cr, Pb, Rb, Th	Cu, Li, Mo, Sc, Zn
SO_3	Sr, U	V	Rb, Hf	Ba, Cr, Mo, Zn
SiO_2		Mo, Pb, U	Ba, Ga, Rb	B, Co, Li, Th, V
TiO_2	Mo		Co, Cr, Ni, Hg, Sc, Th	Ga, Cl
Ash %		Mo	Th, Pb, Ba	B, Co, Cr, Cu, Ga, Li, Ni, Sc, Hg

associations with the clay minerals, K-feldspar, plagioclase, and oxide minerals. There are also very strong, strong and moderate correlations between Co, Cr, Cu, Mo, Pb, Rb, Li, Th and Ba elements. The sulfide and oxide minerals are generally present in the clay matrix in the samples. During the SEM analysis, Ni and Cr-bearing Fe-oxides, Cr-oxides, Rb-bearing Pb-oxides, Cd-bearing sphalerite and Ni and As-bearing pyrites were commonly observed in the Tunçbilek feed coal (Figure 5). Sütcü and Karayiğit (2015) determined Fe (chromite), Mg (magnesiochromite), Ni, and Zn (zincochromite)-bearing chromium minerals, Cr-bearing pyrite, silicate, clay, and phosphate minerals in the Elbistan coal. In addition, Ni-bearing pyrites and Fe-oxides were detected in the Tunçbilek coals (Sütcü et al., 2021). Karayiğit et al. (2019) detected Co in pentlandite [$(Fe,Ni)_9S_8$] in the combustion residues of Tunçbilek power plant. The weak correlations between SO_3, Cr (r=0.35), Cu (r=0.016), and Mo (r=0.22), along with negative correlations between SO_3, Ni (r=-0.19), and Co (r=-0.07) indicate a dominance of oxide and chloride mineral associations. The correlations between Co, Cr, Cu, Mo, Pb, Rb, Li, Th and Ba elements also support the previous studies.

Karayiğit et al. (2000*a*) was determined Cr-oxide, Cu-Zn sulfide, Cu-Zn-Pb sulfide, CuZn-chloride, chromite, galena in the Tunçbilek, Soma-5-6 unit, and Yeniköy feed coals. Karayiğit et al. (2000*a*) suggested that some unusual sulfide and chloride minerals (BiPb-sulfide, CuZn-chloride, NaCl+CuZn-sulfide, and NaCl+CuZnPb-sulfide) in the feed coals probably were formed from pore solutions derived from volcanic material in the Neogene coal basins or they were all derived from a common detrital source through diagenesis. These elements are also redox sensitive and they are soluable in oxic conditions and unsoluable under oxgen-poor conditions. Hill et al. (2024) found elevated concentrations of Al, V, Cr, Cd, U, Mn, Co, Cu, As, and Rb in the phosphate-bearing carbonate fluorapatite mineral phase of young phosphate rocks (Miocene to Late Cretaceous) relative to those of older (Devonian to Precambrian) rocks. Such phosphate formations are commonly observed in the carbonate sequences extending from west to east across southern and southeastern Anatolia, which also represent the basement rocks of the Elbistan, Tufanbeyli, and Yatağan basins.

Arsenic shows a strong correlation with Cl and weaker correlation with Fe_2O_3, Hf, Cd, and B. In the Çan feed coal, the concentrations of As and Cl are higher, while SO_3 is lower compared to other feed coals. The Çan coal basin is settled on the volcanic basement rocks, with its boundaries defined by faults that facilitate the circulation of hydrothermal fluids rich in elements such as As, Cl, Pb, Rb, B, and Zn in the basin. The volcanic rocks and hydrothermal fluids are believed to significantly contribute to the higher concentrations of As and Cl in the Çan feed coal compared to other coals. The As concentration can be mostly related to As-chlorides. On the other hand, As bearing pyrites were detected in the Elbistan coals (Sütcü and Karayiğit, 2015). The Zn concentration in the coals can be related to the sulfide and oxide minerals. Sphalerite, Zn-oxide, and Cd-Zn-Ni ferrite were detected in the feed coals and ashes. The carbonate basement rocks of the Tufanbeyli and Elbistan coal basins that are very close to each host many of the Pb-Zn, iron, bauxite, baryte, and phosphate deposits (Metin, 1983; Ceyhan, 2003; Taş, 2009; Hanilçi et al., 2019). These basins were probably fed by karst waters during and after peat deposition and coalification periods (Sütcü and Karayiğit, 2015). Consequently, the karst waters may have supplied many elements such as Pb, Fe, Zn, and Ba into the coal depositional environment in this region. Whereas it is believed that in Western Anatolia, As-Sb-Pb-Zn mineralizations resulting from volcanic activities in the basement rocks can contribute to the high As, Sb, Zn, and Pb concentrations in the feed coals. Karayiğit et al. (2000*b*) also stated that post-Miocene hydrothermal mineralizations can cause As and Sb enrichments in the Gökler coalfield (Kütahya-Western Anatolia).There are epithermal Ag-As-Pb-Zn and porphyry type Au-Cu mineralizations related to the arc magmatism in the Soma basin and Au, Ag, As, Sb, Cu, Pb, Zn and Mo anomalies in the soil and stream samples were detected during the exploration studies for the As-Ag-Sb-Pb-Zn and Au-Cu mineralizations in the Çatalçam-Soma region (Sarı et al., 2022). The pyrite+chalcopyrite+galena+sphalerite bearing quartz+baryte vein-veinlets were observed in the drilling cores during the exploration studies. In the studied samples, Cl correlates very strongly to As, moderately to Cu, Hf, and Hg, and weakly to Co and Ni. Therefore, chlorides can be the other element source besides sulfide and oxides.

Strontium correlates very strongly and strongly to U, V, CaO, SO_3 and P_2O_5 which indicate association with calcite, phosphate, and sulfate minerals. It is well known that Sr can enter the lattice of calcite, fluorite, and baryte (Barbieri et al., 1984). The moderate and weak correlations between Ba, Cr, Cu, Mo, Rb, Hf, Fe_2O_3, B, Li, Sc, Th, Zn, and Ti indicate As-Cr-Cu-Zn mineralizations, borate, and baryte deposits. Celestine ($SrSO_4$) is present commonly in the borate deposits in Western Anatolia (Helvacı, 2023). Strontium minerals such as celestine and strontianite ($SrCO_3$) are often associated with baryte, Mississipi Valley-Type (MVT) Pb-Zn deposits, and hydrothermal veins in limestones and marls. The correlations between Sr, CaO, and P_2O_5 can also be related to fossil fragments and phosphate minerals. Karayiğit et al. (2000*a*) suggested that Sr is mainly associated with carbonates and sulfates in the Turkish feed coals. Strontium bearing fossil shells and phosphate minerals were observed in the coal series (Querol et al., 1999; Sütcü and Karayiğit, 2015; Sütcü et al., 2021). The fossil fragments in the Elbistan coals contain a high amount of Ca and a trace amount of Fe, Mg, Sr, and Mn (Sütcü and Karayiğit, 2015). The strontium concentrations in young coals with abundant fossil fragments, such as those found in Elbistan, Yatağan, Kemerköy, and Yeniköy, are higher than in other coal basins. In apatite minerals Sr, Ba, and Pb can be substituted for calcium; arsenate and vanadate for phosphate. On the other hand, Querol et al. (1997) showed that Sr and Ba in the Cayirhan lignite have a clear affinity for the zeolite, heulandite.

The uranium concentration of in the feed coals is generally below the detection limit of 10 µg/g therefore correlation coefficients cannot give true relations. However, the U concentrations in the Soma, Kolin, and Tunçbilek feed coals are higher than the World coal average. Uranium correlates very strongly to V and Hg, strongly and moderately to B, Co, Cr, Ga, Li, Ni, Se, Sc, Pb, and Cl. Querol et al. (1999) suggested that the alkaline paleoenvironment gave rise to a peculiar trace element trending which is characterized by the anomalous enrichment of U, Mo and W. These elements are typically fixed under very alkaline conditions and are generally associated with clay minerals, heavy minerals or sulphides. Mo enrichments were observed in the feed coals from the Elbistan, Yatağan, Tufanbeyli, Çayırhan coal basins which have alkaline paleoenvironment conditions. Zielinski and Finkelman (1997) stated that uranium is found in coal's mineral and organic fractions. Cicioğlu (2001) indicated that U concentration in the Elbistan coal can be related to both organic and inorganic matter. Geologically younger and lower-rank coals tend to be enriched in uranium therefore, almost all uranium-rich coals are lignite, and uranium in these low-rank coals is mainly associated with organic matter (Chen et al., 2017). Arbuzov et al. (2011) suggested that the high concentrations of U and Th in coal-bearing deposits are related to the rocks surrounding the basins enriched with U and Th or connected with the occurrence of volcanism during the coal accumulation. Chen et al. (2017) also revealed a similar opinion that genetic factors for uranium enrichment in coal can be related to source rocks, volcanic ashes and magmatic intrusion, hydrothermal fluids, marine waters, ground waters, or organic matter. The highest concentrations of uranium in groundwater are found in areas of known deposits and areas with silicic tuffs and tuffaceous rocks of Oligocene and Miocene age (Denson, 1959). The presence of strong anions such as F^-, Cl^-, $(SO_4)^{2-}$, $(CO_3)^{2-}$, $(PO_4)^{2-}$ increases the solubility and mobility of uranium in groundwater (Cuney and Kyser, 2008). Secondary uranium deposits that are found in caves, solution channels, and fractures in carbonate rocks of karst terrains have been reported (Bell, 1963). Somay (2017) stated that the dominant anion of the waters, except for surface waters, is Cl and the remaining waters are of the Na-Cl water facies type in the Muğla-Yatağan-Bodrum and Aydın-Germencik regions. Additionally, the Elbistan coal basin contains karst aquifers that are rich in carbonate and phosphate ions. Although the feed coals from the Yatağan basin have U concentrations lower than10 µg/g, the bottom ashes and fly ashes from the Kemerköy, Yeniköy, and Yatağan power plants are enriched in uranium. As previously stated, the karstic basement rocks (marble and limestone) and high levels of carbonaceous and phosphatic fossil shells in coal may result in elevated uranium concentrations in the Yatağan and Elbistan basins. Nolan et al. (2021) indicated that uranium (VI) can substitute for calcium in mineral lattices such as apatite, co-precipitate within the calcite mineral lattice, or be contained into dolomite. On the other hand, the concentration coefficients of the Li, Th, U, and V are higher in the feed coals from Kolin and Soma 5-6 unit supplied their coals from the Deniş coalfield where the tuff and agglomerate layers alternate with the coal and clastic layers. Therefore it is thought that the volcanic inputs may also have increased Li, Th, Sr, U, B, and V concentrations. The high U concentrations in the Soma-Torku and Soma-Kolin feed coals support the role of volcanics in increasing the element concentrations. Thorium is associated with monazite which is an accessory mineral in coal and with minor amounts in xenotime, zircon and some clay minerals (Finkelman, 1995). Karayiğit et al. (2000*a*) determined Th-bearing REE phosphates in the feed coals. Sütcü (2021) also determined abundant thorite [$(Th,U)SiO_4$], zircon, and monazite minerals in the fly ashes of Tunçbilek A and B units, Soma-Kolin, Soma-Torku 14 and 56 units. Th and Hf bearing monazite and zircon minerals were detected during the SEM analysis. Arbuzov et al. (2011) also noted that high U and Th concentrations of Paleozoic, Mezosoic, and Cenozoic coals in Siberia, Zabaikalie and Yakutia and eastern Eurasia, are the result of volcanic activities.

Boron very strongly correlates to U, moderately to Li, V, and P_2O_5, weakly to Ba, Co, Pb, Zn, CaO, Na_2O, and TiO_2. The World's largest borate reserves are located in the Western Anatolia. The borate deposits of Turkey were formed in the lacustrine sediments of the Neogene age during periods of volcanic activity. Although the sediments deposited in the borate lakes show some differences, they are generally represented by tuffaceous rocks, claystones, limestones, and Ca, Na, Mg, and Sr-borates (Helvacı, 2015). Thermal springs and hydrothermal solutions associated with volcanic activity are regarded as the most likely source of the boron. In the borate deposits, Na, Cl, SO_4, and CO_2 ions can be carried into the basin by the thermal and mineral waters related to the active volcanism (Helvacı and Ercan, 1993). Although lithium concentrations in Western Anatolia are generally related to volcanic activity, they are particularly enriched in the feed coal from Elbistan and Tufanbeyli. Besides brines, salt lakes, and pegmatite deposits, karst bauxite deposits have also been considered an alternative source of lithium in recent years (Economou-Eliopoulos and Kanellopoulos, 2023). The carbonate basement rocks in both basins contain karst bauxite deposits, indicating that these deposits may be a source of lithium in the Elbistan and Tufanbeyli basins.

3.3.2. Bottom Ashes

The trace element concentrations of the bottom ashes are listed in Table 10. Even though the trace

Table 10- Trace element concentrations of bottom ash samples (µg/g).

Sample No	As	B	Ba	Cd	Co	Cr	Cu	Ga	Li	Mo	Ni	Pb	Rb	Sb	Se	Sr	Hf	Sc	Th	U	V	Zn	Hg	Cl
TA-BA	<10	64	431	<5	47	271	69	13	19	<5	931	13	<10	<10	<5	231	3.2	12.1	30	<10	56	53	0.02	0
TB-BA	<10	26	184	<5	24	92	41	7	15	<5	554	<10	<10	<10	<5	102	2.1	5.1	16	<10	22	24	0.01	100
S14-BA	42	247	390	<5	<5	36	19	9	33	<5	27	<10	17	<10	<5	354	1.1	4.7	13	20	80	62	0.01	0
S56-BA	32	233	624	<5	6	45	24	12	56	<5	24	15	32	<10	<5	287	1	6.3	15	16	112	97	0.014	0
K-BA	20	304	263	<5	6	45	23	10	66	<5	43	19	17	<10	<5	155	0.7	5.5	19	12	153	41	0.006	0
ÇAN-BA	193	156	292	<5	11	18	37	<5	71	<5	36	14	75	<10	<5	292	11.1	8.2	20	12	94	63	0.003	0
ELB -BA	<10	110	409	<5	21	170	51	18	71	11	152	<10	100	<10	<5	559	7.8	10.7	19	<10	234	63	0.004	0
TUF-BA	34	33	572	<5	7	100	24	16	106	5	56	44	133	<10	<5	264	1	9.9	12	11	99	312	0.01	100
YAT-BA	107	171	561	<5	15.2	130	48	20.6	53	20.7	70.6	27	85.8	<10	<5	654	1.7	10.8	24.9	36.7	122	84.2	0.16	50
KEM-BA	22	45	373	<5	13.2	101	37	16.9	62	12.6	51	12	71	<5	<5	1044	1.6	14.6	12.3	49.1	193	56	0.0013	0
YEN-BA	20	52	335	<5	13.7	96	35	16.6	68	9.8	53	10	74	<5	<5	643	1.5	4.4	10.7	39.9	166	50	0.0002	100
ÇAT-BA	<10	18	321	<5	<5	47.2	23	<5	13.1	13.1	14.7	<10	25	<10	<5	108	0.9	2.2	<10	<10	21.1	<10	0	0
WC	7.6	56	150	0.2	4.2	15	15	5.5	10	2.2	9	6.6	10	0.84	1	120	1.2	4.1	3.3	2.9	22	18	0.1	120
WCA	48	410	900	1.1	26	82	74	29	49	15	52	38	48	5	7.6	740	7.5	23	19	16	140	110	0.62	770
Concentration Coeffient (CC)																								
TA-BA	-	0.2	0.5	-	1.8	3.3	0.9	0.4	0.4	-	17.9	0.3	-	-	-	0.3	0.4	0.5	1.6	-	0.4	0.5	0.0	0.0
TB-BA	-	0.1	0.2	-	0.9	1.1	0.6	0.2	0.3	-	10.7	-	-	-	-	0.1	0.3	0.2	0.8	-	0.2	0.2	0.0	0.1
S14-BA	0.9	0.6	0.4	-	-	0.4	0.3	0.3	0.7	-	0.5	-	0.4	-	-	0.5	0.1	0.2	0.7	1.3	0.6	0.6	0.0	0.0
S56-BA	0.7	0.6	0.7	-	0.2	0.5	0.3	0.4	1.1	-	0.5	0.4	0.7	-	-	0.4	0.1	0.3	0.8	1.0	0.8	0.9	0.0	0.0
K-BA	0.4	0.7	0.3	-	0.2	0.5	0.3	0.3	1.3	-	0.8	0.5	0.4	-	-	0.2	0.1	0.2	1.0	0.8	1.1	0.4	0.0	0.0
ÇAN-BA	4.0	0.4	0.3	-	0.4	0.2	0.5	-	1.4	-	0.7	0.4	1.6	-	-	0.4	1.5	0.4	1.1	0.8	0.7	0.6	0.0	0.0
ELB -BA	-	0.3	0.5	-	0.8	2.1	0.7	0.6	1.4	0.7	2.9	-	2.1	-	-	0.8	1.0	0.5	1.0	-	1.7	0.6	0.0	0.0
TUF-BA	0.7	0.1	0.6	-	0.3	1.2	0.3	0.6	2.2	0.3	1.1	1.2	2.8	-	-	0.4	0.1	0.4	0.6	0.7	0.7	2.8	0.0	0.1
YAT-BA	2.2	0.4	0.6	-	0.6	1.6	0.6	0.7	1.1	1.4	1.4	0.7	1.8	-	-	0.9	0.2	0.5	1.3	2.3	0.9	0.8	0.3	0.1
KEM-BA	0.5	0.1	0.4	-	0.5	1.2	0.5	0.6	1.3	0.8	1.0	0.3	1.5	-	-	1.4	0.2	0.6	0.6	3.1	1.4	0.5	0.0	0.0
YEN-BA	0.4	0.1	0.4	-	0.5	1.2	0.5	0.6	1.4	0.7	1.0	0.3	1.5	-	-	0.9	0.2	0.2	0.6	2.5	1.2	0.5	0.0	0.1
ÇAT-BA	-	0.04	0.4	-	-	0.6	0.3	-	0.3	0.9	0.3	-	0.5	-	-	0.1	0.1	0.1	-	-	0.2	-	0.0	0.0

element concentrations are higher than the feed coals, most of the trace elements are in the range of normal or depleted levels compared to the World coal ash averages (Ketris and Yudovich, 2009). Only Ni, As, Cr, Rb, and U are enriched in some bottom ashes. Nickel is significantly enriched only in the Tunçbilek A and B units. Arsenic is slightly enriched in the Çan and Yatağan bottom ashes. The Elbistan bottom ash shown slight enrichment in Cr and Rb. Cromium is also enriched in Tunçbilek A unit. Uranium is slightly enriched in the Yatağan, Kemerköy, and Yeniköy bottom ashes. The Tufanbeyli bottom ash is slightly enriched in Li, Rb, and Zn. According to the Pearson correlation coefficients, Ni very strongly correlates to MgO and Co, strongly to Fe_2O_3, Cr, and Cu, moderately to SiO_2, U, and Rb, and weakly to Sc (Table 11). There are also very strong and strong correlations between Co, Cr, Cu, Ni, Mo, Th and Fe_2O_3. Mg bearing siderites, Ni and Cr bearing Fe-oxides were commonly observed in the Tufanbeyli and Kolin fly ashes during the SEM analysis (Figure 4a). Cd-Ni-Zn-ferrites were also detected in some feed coals with the XRD analysis. As stated before, Fe and Mg may substitute for Ni. Hence, the very strong and strong correlations between Ni, MgO and Fe_2O_3 can be related to the Mg bearing Fe-oxides and siderites, dolomites and Cd-Ni-Zn-ferrite. These minerals can be the sources of Ni concentrations in the ashes (Figure 4b).

Rubidium is strongly correlated to Cr, Ga, Li, Pb, Sc, Zn, and Cl, moderately to P_2O_5, Cu, and Ni, and weakly to As, Hf, V, Fe_2O_3, SO_3, and TiO_2 as in the feed coals. These correlations indicate the associations with Pb-oxides, and phosphate minerals in the bottom ashes. On the other hand, the strong correlation with Cl indicates the presence of chlorides.

Rubidium-bearing Pb-oxides have been observed in the feed coals and fly ashes. Lithium is very strongly correlated to SO_3 and Cr, strongly to Rb, Zn, and V, moderately to CaO, P_2O_5, and Ga, and weakly to Ba, Sr, Hf, Sc, Cl, and TiO_2. Therefore, Li can be associated with carbonate, sulfate and phosphate minerals. Cromium is very strongly correlated to Co, Cu, and Li, strongly to Ni, Rb, Sc, Th, U, and Fe_2O_3, moderately to MgO and SiO_2, and weakly to Ga, Hg, and P_2O_5. The Cr concentration in the bottom ashes can be related to the chromite and Cr- and Fe-oxides and glass phases (Figure 4a). Sütcü and Karayiğit (2015) detected Fe and Mg-bearing chromite in the Elbistan coal. Karayiğit et al. (2000*a*) determined chromite and Cr-oxides in the feed coals of the Tunçbilek, Soma, and Yeniköy power plants. Arsenic is very strongly correlated to Mo and Hf, strongly to Th, moderately to Cu, Ga, and SiO_2, and weakly to SO_3, TiO_2, Fe_2O_3, Hg, Rb and Co. Although, arsenic is very strongly correlated to Cl (r =0.85) in the feed coals, there is a negative weak correlation between As and Cl. Hence, As can be associated with the glass phase and Fe-oxides in the bottom ashes due to its moderate correlation with SiO_2, weak correlation with Fe_2O_3. Querol et al. (1995) stated that elements with sulfide and organic affinities are oxidized during

Table 11- Pearson correlations between major oxides and trace elements of the bottom ash samples.

	0.8<r<1 Very strong	0.6<r<0.79 strong	0.4<r<0.59 moderate	0.2<r<0.39 weak
Al_2O_3		SiO_2	TiO_2	Fe_2O_3, Na_2O, Ni, Th
CaO			P_2O_5, SO_3, B, Li, Sr, V	Ba
Fe_2O_3	Mo	SiO_2, MgO, Co, Cr, Cu, Ni, Th	U, Hg	Al_2O_3, K_2O, Rb, As, Sc,
K_2O	U		SiO_2	Fe_2O_3, TiO_2, Co, Ga, Mo
MgO	Co, Ni	Fe_2O_3	SiO_2, P_2O_5, Cr, Cu, Mo, U	Cl, Th
Na_2O	U	Ga		Al_2O_3, SiO_2, Mo, Sr
P_2O_5	U, V	Sr	CaO, MgO, Ga, Li, Rb, Sc	Cr, Cu, Hf
SO_3	Li		CaO, V, Zn	As, B, Pb, Rb, Hf
SiO_2		Fe_2O_3, Al_2O_3, Th	K_2O, MgO, As, Cu, Mo, Ni	Ti
TiO_2	Pb	Zn	Al_2O_3	SiO_2, K_2O, NaO, SO_3, As, Ga, Li, Rb

coal combustion. Consequently, they may show volatile behavior because of the temperature rise accompanying oxidation or as a result of reactions with Cl, F, Na, or S compounds which can induce volatility in some elements such as As, Se, and Cd. Even if these trace elements are not volatilized, they are present in the ash mainly in oxides and sulfates. The concentration of Cl in the bottom ashes is lower than in the feed coals due to its volatile characteristics. It is generally found in the ashes as water-soluble chlorides [KCl, NaCl, and $CaCl_2 \cdot 2H_2O$ with the less soluble Ca(OH)Cl (Pedziwiatr et al., 2021)].

It seems that uranium was concentrated in the bottom ashes after combustion compared to the feed coals, which can be related to the association with organic matter in the feed coals. Uranium is very strongly correlated to Co, Sr, K_2O, Na_2O, and P_2O_5, strongly correlated to SiO_2, Cr, Cu, Ga, V, and Hg, moderately to Mo, Ni, Sc, and Fe_2O_3, and weakly to Hf. The very strong and strong correlations with K_2O, Na_2O, SiO_2, and P_2O_5 can be related to K-feldspars, glass phases, and phosphate minerals and moderate correlation with Fe_2O_3 also indicate Fe-oxides and Fe-bearing carbonate minerals such as dolomite and siderite. The strong correlations between U, Cr, Cu, and Ga can be related to Fe-oxide associations. Vanadium and Sr that correlate very strongly to U were commonly observed in the plagioclase and glassy phases (V), and phosphate minerals (Sr) during the SEM analysis. Uranium can also be associated with thorite minerals which are commonly observed in the Tunçbilek, Soma-Torku and Kolin fly ashes. Palmer et al. (2004) stated that the average uranium concentrations of the Turkish coals generally increase from north to south in Western Türkiye. This case is observed in the studied samples. For instance, the Yatağan, Yeniköy, and Kemerköy bottom ashes have higher U concentrations than the Çan, Soma-Torku, and Soma-Kolin bottom and fly ashes.

3.3.3. Fly Ashes

The trace element concentrations of the fly ashes are listed in Table 12. The trace element concentrations in coal ashes are generally within the normal or depleted ranges compared to the averages reported by Ketris and Yudovich (2009). However, some trace elements are enriched in the studied fly ashes. Nickel is significantly enriched and enriched in both the Tunçbilek A and B units. Additionally, Cr shows slight enrichment in the Tunçbilek ashes. The Soma 1-4 unit fly ash is slightly enriched in As and U. The Kolin fly ash is slightly enriched in B, Li, U, and V. The Çan fly ash is only significantly enriched in As. The Elbistan fly ash is slightly enriched in Cr, Ni, and Rb. The Tufanbeyli fly ash is enriched in Cd and slightly enriched in U and Zn. The Çayırhan fly ash is slightly enriched in As and Ni. The Yatağan fly ash is slightly enriched in As, Rb, U. The Kemerköy fly ash is only enriched in U and the Yeniköy is enriched Rb and U. The trace element concentrations in the Çatalağzı fly ash are in the range of normal or depleted levels. Pearson correlation coefficients between major oxides and trace elements of the fly ashes are listed in Table 13. Nickel can be associated with Fe-oxides, Fe-carbonates, glass phases, mullite, and plagioclases due to its very strong correlation with Hg, strong with U, MgO, and SiO_2, and moderate with Rb, Se, Al_2O_3, and Fe_2O_3. Cr is very strongly correlated to Se, strongly to Hf, moderately to Ni, Rb, U, and MgO, and weakly to Hg, Fe_2O_3, and SiO_2. Therefore, Cr is probably present in fly ashes as oxides such as magnesioferrite, Cr-oxide, and Cr-Fe-oxide or within carbonate minerals such as siderite and dolomite. Nickel and Cr bearing Fe-oxides and glass phases were detected in the fly ashes during the SEM analyses (Figure 4a and b).

Rubidium can be associated with phosphate minerals and Fe-oxides related to the strong correlations with Se, Hf, and P_2O_5, moderately with Co, Cr, Ni, and Fe_2O_3, and weakly with Cu, Sc, MgO, and Na_2O. On the other hand, Hf bearing zircon minerals were commonly observed in the fly ashes. Arsenic is moderately correlated to Fe_2O_3, weakly to Cu, Li, Mo, Th, Na_2O, and TiO_2 hence it can be associated with Fe-oxides. Due to its volatile characteristics As is enriched in fly ashes and depleted in the bottom ashes. Cadmium and Zn are only enriched in Tufanbeyli fly ash. The Zn concentration is also higher in the Tufanbeyli, Elbistan, and Çatalağzı feed coals. As it was stated previously, Zn is present as sphalerite, Zn-oxide, and Cd-Zn-Ni ferrite in the feed coals. The SEM analysis showed that sphalerite mineral partially transformed into Zn-carbonate after combustion in the

Table 12- Trace element concentrations of the fly ashes and their concentration coefficients (CC) (µg/g).

Sample No	As	B	Ba	Cd	Co	Cr	Cu	Ga	Li	Mo	Ni	Pb	Rb	Sb	Se	Sr	Hf		Sc	Th	U	V	Zn	Hg	Cl
TA-FA	33	143	446	<5	32	170	47	9	15	8	762	<10	<10	<10	<5	172	2.3		8.4	21	<10	66	36	0.4	0
TB-FA	38	114	334	<5	19	174	31	7	14	7	379	<10	<10	<10	<5	189	2		5.9	14	<10	46	33	0.1	0
S14-FA	127	644	632	<5	8	59	29	15	57	<5	32	25	29	<10	<5	459	1.1		7.7	18	35	152	56	0.1	100
S56-FA	73	320	794	<5	7	57	28	15	64	<5	33	21	37	<10	8	324	0.2		7.5	16	18	140	71	0.1	0
K-FA	59	1756	435	<5	22	128	54	22	116	<5	86	36	44	<10	11	346	0.8		14	33	62	670	79	0.1	100
ÇAN-FA	781	326	287	<5	15	16	55	8	93	<5	25	28	82	<10	<5	332	<0.1		8.6	27	20	156	71	0	0
ELB -FA	12	105	375	<5	19	166	44	8	56	13	131	18	128	<10	<5	590	6.9		9.2	23	<10	207	62	0	0
TUF-FA	91	76	587	7	13	152	33	20	82	19	89	24	72	<10	11	307	3.8		12	22	32	172	473	0	100
ÇAY-FA	213	620	336	<5	12	138	16	11	12	10	180	20	<10	<10	11	391	2.3		6.8	19	<10	64	65	0.027	100
YAT-FA	144	179	574	<5	16	136	49	22	54	19	71	14	102	<10	<5	662	3		11	24	35	123	94	0	0
KEM-FA	59	47	335	<5	14	96	35	19	68	14	49	23	90	<5	<5	982	1.4		15	12	38	186	87	0	0
YEN-FA	55	54	298	<5	14	102	33	20	78	12	51	26	99	<5	<5	654	1.5		15	12	36	180	83	0	0
ÇAT-FA	35	65.1	554	<5	<5	26	26	<5	17	12	15	11	<10	<10	<5	147	<0.1		2.3	<10	<10	39	22	0.2	10
WCA	48	410	900	1.1	26	82	74	29	49	15	52	38	48	5	7.6	740	7.5		23	19	16	140	110	0.62	770
WBCA	46	260	980	1.2	37	120	110	36	82	14	100	55	110	7.5	7.6	730	9		24	23	15	170	170	0.87	2100
Concentration coefficient																									
TA-FA	0.7	0.3	0.5	-	1.2	2.1	0.6	0.3	0.3	0.5	14.7	-	-	-	-	0.2	0.3		0.4	1.1	-	0.5	0.3	0.6	0.0
TB-FA	0.8	0.3	0.4	-	0.7	2.1	0.4	0.2	0.3	0.5	7.3	-	-	-	-	0.3	0.3		0.3	0.7	-	0.3	0.3	0.1	0.0
S14-FA	2.6	1.6	0.7	-	0.3	0.7	0.4	0.5	1.2	-	0.6	0.7	0.6	-	-	0.6	0.1		0.3	0.9	2.2	1.1	0.5	0.1	0.1
S56-FA	1.5	0.8	0.9	-	0.3	0.7	0.4	0.5	1.3	-	0.6	0.6	0.8	-	1.1	0.4	0.0		0.3	0.8	1.1	1.0	0.6	0.2	0.0
K-FA	1.2	4.3	0.5	-	0.8	1.6	0.7	0.8	2.4	-	1.7	0.9	0.9	-	1.4	0.5	0.1		0.6	1.7	3.9	4.8	0.7	0.2	0.1
ÇAN-FA	16.3	0.8	0.3	-	0.6	0.2	0.7	0.3	1.9	-	0.5	0.7	1.7	-	-	0.4	-		0.4	1.4	1.3	1.1	0.6	0.0	0.0
ELB -FA	0.3	0.3	0.4	-	0.7	2.0	0.6	0.3	1.1	0.9	2.5	0.5	2.7	-	-	0.8	0.9		0.4	1.2	-	1.5	0.6	0.0	0.0
TUF-FA	1.9	0.2	0.7	6.4	0.5	1.9	0.4	0.7	1.7	1.3	1.7	0.6	1.5	-	1.4	0.4	0.5		0.5	1.2	2.0	1.2	4.3	0.0	0.1
ÇAY-FA	4.4	1.5	0.4	-	0.5	1.7	0.2	0.4	0.2	-	3.5	0.5	-!	-	-	0.5	-		0.3	1.0	-	0.5	0.6	0.0	0.1
YAT-FA	3.0	0.4	0.6	-	0.6	1.7	0.7	0.7	1.1	1.3	1.4	0.4	2.1	-	-	0.9	0.4		0.5	1.2	2.2	0.9	0.9	0.0	0.0
KEM-FA	1.2	0.1	0.4	-	0.5	1.2	0.5	0.6	1.4	1.0	0.9	0.6	1.9	-	-	1.3	0.2		0.6	0.6	2.4	1.3	0.8	0.0	0.0
YEN-FA	1.1	0.1	0.3	-	0.6	1.2	0.4	0.7	1.6	0.8	1.0	0.7	2.1	-	-	0.9	0.2		0.6	0.6	2.2	1.3	0.8	0.0	0.0
ÇAT-FA	0.8	0.3	0.6	-	-	0.2	0.2	-	0.2	0.8	0.1	0.2	-	-	-	0.2	-		0.1	-	-	0.2	0.1	0.3	0.0

WCA: World coal ash average, WBCA: World bituminous coal ash average.

Table 13- Pearson correlations between major oxides and trace elements of the fly ash samples.

	0.8<r<1 Very strong	0.6<r<0.79 strong	0.4<r<0.59 moderate	0.2<r<0.39 weak
Al_2O_3			SiO_2, Ni, Hg	MgO, Fe_2O_3, Co, Pb
CaO		SO_3	Na_2O, P_2O_5, Li, Mo, Sr	Ba, Ga, Hf, Cl, Sc
Fe_2O_3		Se	SiO_2, As, Co, Ni, Rb	Al_2O_3, Cr, Hf
K_2O		MgO, Na_2O	Sr, Ga, Sc	SiO_2
MgO	P_2O_5, SO_3	K_2O, Ni	Co, Cr, Hg	Al_2O_3, Rb
Na_2O		K_2O, Sr	CaO, Ga, Sc	As, Li, Mo, Rb
P_2O_5	MgO	Rb, Sr, Hf	CaO	Na_2O, Sc
SO_3	Se	Zn	CaO, Li, Mo, Sc, Cl	P_2O_5, B, Ga, Pb, Hf, Th, U, V
SiO_2		Al_2O_3, Ni, Hg	Co, Fe_2O_3, MgO	Na_2O, K_2O, Cr
TiO_2	Th	B, V	Cu, Cl	P_2O_5, As, Ba, Ga, Li, Pb, Se, U

coal ashes (Figure 4c). In the ash samples, sphalerite and Zn-oxides were detected in both XRD and SEM analyses. Cadmium bearing sphalerites were also observed during the SEM analyses. The elements As, B, Cd, Pb, and Zn in the feed coals could easily become volatile during combustion; these elements are retained in fly ash. The CaO in the fly ash tends to retain As, B, and Hg (Querol et al., 1995; Meij and Te Winkel, 2006; Kostova et al., 2016). Similarly, B, Cd, Zn, and As, which were retained by Ca, were also enriched in the studied fly ashes as oxides or sulfates.

Uranium is more concentrated in the finer-sized (-38µ grain size) particles in the fly ashes (Sütcü, 2021). Uranium is very strongly correlated to V and Hg, strongly to B, Co, Ga, Ni, Se, Sc, moderately to Cr, Li, Pb, and Cl, and weakly to Cu, Th, SO_3, and TiO_2. The weak correlations with major oxides indicate the associations of oxides, sulfates, and chlorides such as thorite, B-oxides, Fe-oxides, B-chlorides for uranium in the fly ashes. Thorite [$(Th,U)SiO_4$] mineral was commonly observed in the Tunçbilek, Soma-Torku, and Soma-Kolin fly ashes in the mineral liberation analyses (MLA) analyses (Sütcü, 2021). Vanadium-bearing anorthites, glass phases and carbonates are also present in the Tufanbeyli and Soma-Kolin fly ashes (Figure 5d). On the other hand, it is believed that V is probably associated with B-oxides due to the very strong correlation between B and V in the fly ashes. Furthermore, the strong correlation between U, V, and B supports the association with B-oxides. Lithium is strongly correlated to Mo, Pb, Sc, and V, moderately to B, Cu, Ga, U, Th, CaO, and SO_3, and weakly to As, Ti, Zn, Sr, Se, Na_2O. The moderate correlations with B, CaO and SO_3 indicate sulfates and boron minerals in the fly ashes. Therefore, Li can be associated with sulfate, oxide, and carbonate minerals. Boron is very strongly correlated to V, strongly to Pb, Th, U, Cl, TiO_2, moderately to Li, and weakly to Cu, Ga, Se, and SO_3. These correlations indicate the B-chlorides, B-oxides, and sulfate minerals.

4. Conclusion

The mineral compositions and element concentrations of the feed coals show differences related to the geological characteristics of the coal basins from where they were supplied. The feed coals mostly contain quartz, clay minerals (kaolinite, vermiculite, and illite), calcite, dolomite, plagioclase, K-feldspar, and pyrite minerals. Additionally, smectite, siderite, gypsum, zeolite, sphalerite, magnesioferrite, and mica minerals are present in some feed coals. During combustion, most of the minerals are converted into different mineral phases. Therefore, bottom and fly ashes have different mineral compositions compared to the feed coals. The main components of the ashes are generally represented by glass phases, quartz, calcite, dolomite, anhydrite, portlandite, magnesite, lime, gypsum, plagioclase, hematite, magnetite, mullite, and spinels. The feed coals from the basins having volcanic inputs are rich in K-feldspar and zeolite group minerals, while coals from basins with carbonate basement rocks contain abundant carbonate and phosphate minerals. In the feed coals, As, B, Ba, Co, Cr, Cu, Li, Mo, Ni, Pb, Rb, Se, Sr, Hf, Sc, Th, U, V, and Zn are enriched related to the ore mineralizations in the basement rocks, volcanic inputs, hydrothermal fluids, karst and meteoric waters in the coal basins. Many element concentrations are depleted in the bottom and fly ashes compared to the feed coals. However, As, Cr, Ni, Zn, Li, Rb, and U in some bottom ashes, and As, B, Cd, Cr, Li, Ni, Rb, U, V, and Zn in some fly ashes are enriched. It was observed that siderophile and chalcophile elements such as Ni, Zn, Pb, and Cd are generally associated with iron oxides, spinels, or metal carbonates in coals and coal ashes. In contrast, lithophile elements such as Li, U, B, Th, Ba, Sr, and V are typically present within carbonates, borates, sulfates, oxides, or organic matter in coals, whereas, in the ashes, they are more commonly associated with glass phases, carbonates, and sulfates. It is believed that the high concentrations of Ni, Cd, As, Rb, V, U, and Zn elements in the coal ashes make the ashes an alternative element source.

Acknowledgement

This research was supported by the General Directorate of Mineral Research and Exploration (MTA) (Project no: 2020-35-16-01-4). The authors would like to thank the management of the MTA for their support, and the Turkish Coal Enterprises, Tunçbilek, Soma-Torku, Soma-Kolin, Çan 18 Mart, Elbistan B, Çayırhan, Tufanbeyli, Kemerköy, Yeniköy, Yatağan, and Çatalağzı Power Plant managements and staffs for sampling. We are also grateful to the Mineral Analysis and Technology Department staff of MTA for conducting the elemental analysis, and to Ufuk KİBAR for performing the SEM analysis. Finally, the authors express their gratitude to the editors and the anonymous reviewers for their constructive criticisms.

References

Arbuzov, S. I., Volostnov, A. V., Rikhvanov, L. P., Mezhibor, A. M., Ilenok, S. S. 2011. Geochemistry of radioactive elements (U, Th) in coal and peat of northern Asia (Siberia, Russian Far East, Kazakhstan, and Mongolia). International Journal of Coal Geology 86, 318-328.

ASTM C 618-22. Standard Specification for Coal Fly Ash and Raw or Calcined Natural Pozzolan for Use in Concrete. ASTM International, West Conshohocken, PA, 2018, www.astm.org.

ASTM D2013 / D2013M-18. Standard Practice for Preparing Coal Samples for Analysis. ASTM International, West Conshohocken, PA, 2018, www.astm.org

Aykaç, S., Gürer, A., Çelik, İ., Yıkmaz, B., Eryılmaz, E., Apatay, E., Özdemir, S. A., Gündüz, S., Postacı Can, T., Ak, E., Izladı, E., Erden, S., Özerk, Z. R., Güney, R., Köse, E. B., Demirci, B. B. 2023. Determination of the coal-bearing zones and the alteration zones containing uranium ore by using two dimensional (2D) seismic reflection method in Thrace Basin. Bulletin of the Mineral Research and Exploration 170, 175-192.

Baba, A., Gürdal, G. Yüksel, D. S. 2016. Enrichment of trace element concentrations in coal and its combustion residues and their potential environmental and human health impact: Can Coal Basin, NW Turkey as a case study. International Journal of Environmental Technology and Management 19, 455-480.

Barbieri, M., Masi, U., Tolomeo, L. 1984. Strontium geochemical evidence for the origin of the barite deposits from Sardinia, Italy. Economic Geology 79, 1360–1365.

Bell, K. G. 1963. Uranium in Carbonate Rocks. Geological Survey Professional Paper 474-a. US Goverment Priting Office, Washington, 20.

Bozkurt, E., Mittwede, S. K. 2001. Introduction: Evolution of continental extensional tectonics of western Turkey. Geodinamica Acta 18, 153-165.

Chen, J., Chen, P., Yao, D., Huang, W., Tang, S., Wang, K., Liu, W., Hu, Y., Zhang, B., Sha, J. 2017. Abundance, Distribution, and Modes of Occurrence of Uranium in Chinese Coals. Minerals 7, 239.

Ceyhan, N. 2003. Lead Isotope Geochemistry of Pb-Zn Deposits from Eastern Taurides, Turkey. MSc Thesis, Middle East Technical University, 90, Ankara (unpublished).

Cicioğlu, E. 2001. Investigation of geochemical properties of Çöllolar-Kışlaköy lignites. (Afşin–Elbistan). PhD Thesis, Hacettepe University, 174, Ankara (unpublished).

Cina, A. 1990. Sulphide and arsenide mineralization with the basic and ultrabasic rocks of Albanian ophiolites. In: Malpas, Panayiotou, Panayiotou, Xenophontos (Eds.), Ophiolites; Oceanic Crustal Analogues; Proceedings of the Symposium Troodos 1987, Nicosia, Cyprus, 615– 626.

Çöteli, M., Albayrak, M., Kibar, U., Yavuz, A., Turgut, G., Karahan, D. S. 2025. Mineralogical examination of biomass ashes: a preliminary study for potassium enrichment and phosphoric acid $H_3 PO_4$ production. Bulletin of the Mineral Research and Exploration 176, 57-75. https://doi.org/10.19111/bulletinofmre.1555249

Cuney, M., Kyser, K. 2008. Recent and not-so-recent developments in uranium deposits and implications for exploration. Mineralogical Association of Canada Short Course Series 39, 271.

Dai, S., Li, D., Chou, C. L., Zhao, L., Zhang, Y., Ren, D., Ma, Y., Sun, Y. 2008. Mineralogy and geochemistry of boehmite-rich coals: new insights from the Haerwusu Surface Mine, Jungar Coalfield, Inner Mongolia, China. International Journal of Coal Geology 74, 185–202.

Dai, S., Ren, D., Chou, C. L., Finkelman, R. B., Seredin, V. V., Zhou, Y. 2011. Geochemistry of trace elements in Chinese coals: a review of abundances, genetic types, impacts on human health, and industrial utilization. International Journal of Coal Geology 94, 3-21.

Dai, S., Seredin, V. V., Ward, C. R., Hower, J. C., Xing, Y., Zhang, W., Song, W., Wang, P. 2015. Enrichment of U–Se–Mo–Re–V in coals preserved within marine carbonate successions: geochemical and mineralogical data from the Late Permian Guiding Coalfield, Guizhou, China. Mineralium Deposita 50, 159–186.

Dai, S., Liu, J., Ward, C. R., Hower, J. C., French, D., Jia, S., Hood, M. M., Garrison, T. M. 2016. Mineralogical and geochemical compositions of Late Permian coals and host rocks from the Guxu Coalfield. Sichuan Province, China, with emphasis on enrichment of rare metals. International Journal of Coal Geology 166. 71–95.

Dai, S., Yan, X., Ward, C. R., Hower, J. C., Zhao, L., Wang, X., Zhao, L., Ren, D., Finkelman, R. B. 2018. Valuable elements in Chinese coals: a review. International Geology Review 60, 590-620.

Demir, I., Hughes, R. E., DeMaris, P. J. 2001. Formation and use of coal combustion residues from three types of power plants burning Illinois coals. Fuel 80, 1659–1673.

Denson, N. M., Bachman, G. O., Zeller, H. D. 1959. Uranium-bearing lignite in Northwestern South Dakota and adjacent states. U.S. Geological Survey Bulletin 1055-B, 11–57.

Du, G., Zhuang, X., Querol, X., Izquierdo, M., Alastuey, A., Moreno, T., Font, O. 2009. Ge distribution in the Wulantuga high-germanium coal deposit in the Shengli coalfield, Inner Mongolia, northeastern China. International Journal of Coal Geology 78, 16–26.

Economou-Eliopoulos, M., Kanellopoulos, C. 2023. Abundance and Genetic Significance of Lithium in Karst-Type Bauxite Deposits: A Comparative Review. Minerals 13, 962.

Enerji Atlası. https://www.enerjiatlasi.com/ 12th August 2024.

EPA Method 5050. Bomp preparation method for solid waste. https: //www.epa.gov/sites/production/files/2015-12/documents/5050.pdf

EPA Method 7473. Mercury in solids and solutions by thermal decomposition, amalgamation, and atomic absorption spectrophotometry. https://www.epa.gov/sites/default/files/2015-07/documents/epa-7473.pdf

Finkelman, R. B. 1995. Modes of Occurrence of Environmentally-Sensitive Trace Elements in Coal. In: Swaine, D. J., Goodarzi, F. (eds) Environmental Aspects of Trace Elements in Coal. Energy & Environment 2, Springer, Dordrecht, 20-50.

Franus, W., Wiatros-Motyka, M. M., Wdowin, M. 2015. Coal fly ash as a resource for rare earth elements. Environmental Science and Pollution Research 22, 9464–9474.

Güleç, N., Erler, A. 1983. Trace elements characteristics of pyrites in sulfide massive deposits of Turkey and Cyprus. Bulletin of Geolgical Society 26, 145–152.

Gürdal, G. 2008. Geochemistry of trace elements in Çan coal (Miocene), Çanakkale, Turkey. International Journal of Coal Geology 74, 28–40.

Hanilçi, N., Öztürk, H., Kasapçı, C. 2019. Carbonate-Hosted Pb-Zn Deposits of Turkey. In: Pirajno, F., Ünlü, T., Dönmez, C., Şahin, M. B. (eds) Mineral Resources of Turkey. Modern Approaches in Solid Earth Sciences 16. Springer. 749.

Helvacı, C. 2015. Geological features of Neogene basins hosting borate deposits: an overview of deposits and future forecast, Turkey. Bulletin of the Mineral Research and Exploration 151, 169–215.

Helvacı, C. 2019. Turkish Borate Deposits: Geological Setting, Genesis and Overview of the Deposits. In: Pirajno, F., Ünlü, T., Dönmez, C., Şahin, M. (eds) Mineral Resources of Turkey. Modern Approaches in Solid Earth Sciences 16. Springer, 749.

Helvacı, C. 2023. Geological Features of Neogene Basins Hosting Borate Deposits: An Overview of Deposits and Future Forecast, Turkey. Bulletin of the Mineral Research and Exploration 151, 169-215.

Helvacı, C., Ercan, T. 1993. Recent borate salts and associated volcanism in the Karapınar Basin (Konya), Turkey 46. Türkiye Jeoloji Kurultayı Bildiri Özleri,15-19 Şubat 1993, Ankara, 102–103.

Hill, R. C., Wang, Z., Williams, G. D. Z., Polyak, V., Singh, A., Kipp, M. A., Asmerom, Y., Vengosh, A. 2024. Reconstructing the depositional environment and diagenetic modification of global phosphate deposits through integration of uranium and strontium isotopes, Chemical Geology 662, 122214.

Hower, J. C. 2012. Petrographic examination of coal-combustion fly ash, International Journal of Coal Geology 92, 90-97.

Hower, J. C., Trimble, A. S., Eble, C. F., Palmer, C. A., Kolker, A. 1999. Characterization of fly ash from low-sulfur and high-sulfur coal sources: partitioning of carbon and trace elements with particle size. Energy Sources 21, 511–525.

Hower, J. C., Granite, E. J., Mayfield, D. B., Lewis, A. S., Finkelman, R. B. 2016. Notes on contributions to the science of rare earth element enrichment in coal and coal combustion by-products. Minerals 6, 32.

Höll, R., Kling, M., Schroll, E. 2007. Metallogenesis of germanium-review. Ore Geology Reviews 30, 145-180.

Kalyoncu Ergüler, G., Bayındır, F. M., Dağlıyar, A. 2021. Investigation of the effect of fly ash released from Kütahya thermal power plants by using remote sensing methods. Bulletin of the Mineral Research and Exploration 166, 1-18.

Karayiğit, A. I., Çelik, Y. 2003. Mineral matter and trace elements in Miocene coals of the Tuncbilek-Domanic Basin, Kutahya, Turkey. Energy Sources 25, 339-355.

Karayiğit, A. I., Gayer, R. A., Querol, X., Onacak, T. 2000*a*. Contents of major and trace elements in feed coals from Turkish coal-fired power plants. International Journal of Coal Geology 44, 169–184.

Karayiğit, A. I., Spears, D. A., Booth, C. A. 2000*b*. Antimony and arsenic anomalies in the coal seams from the Gokler coalfield, Gediz, Turkey. International Journal of Coal Geology 44, 1–17.

Karayiğit, A. I., Onacak, T., Gayer, R. A., Goldsmith, S. 2001. Mineralogy and geochemistry of feed coals and their combustion residues from the Cayirhan power plant, Ankara, Turkey. Applied Geochemistry 16, 911-919.

Karayiğit, A. İ., Yiğitler, Ö., İşerli, S., Querol, X., Mastalerz, M., Oskay, R. G., Hower, J. C. 2019. Mineralogy and geochemistry of feed coals and combustion residues from Tunçbilek and Seyitömer coal-fired power plants in western Turkey. Coal Combustion and Gasification Products 11, 18-31.

Ketris, M. P., Yudovich, Ya. E. 2009. Estimations of Clarkes for Carbonaceous biolithes: world averages for trace element contents in black shales and coals. International Journal of Coal Geology 78, 135–148.

Kostova, I., Vassileva, C., Dai, S., Hower, J. C. 2016. Mineralogy, geochemistry and mercury content characterization of fly ashes from the Maritza 3 and Varna thermoelectric power plants, Bulgaria. Fuel 186, 674-684.

Lin, R., Howard, B. H., Roth, E. A., Bank, T. L., Granite, E. J., Soong, Y. 2017. Enrichment of rare earth elements from coal and coal by-products by physical separations. Fuel 200, 506–520.

Mardon, S. M., Hower, J. C. 2004. Impact of coal properties on coal combustion byproduct quality: examples from a Kentucky power plant. International Journal of Coal Geology 59, 153–169.

Meij, R., Te Winkel, H. 2006. Mercury emissions from coal-fired power stations: the current state of the art in the Netherlands. Science Total Environment 368, 393–396.

Metin, S. 1983. The geology of an area amongst the Derebaşı (Develi), Armutalan and Gedikli (Saimbeyli) villages in the Eastern Tauride Mountains. Yerbilimleri Dergisi 4, İTÜ, 1-2.

Nesse, W. D. 2000. Introduction to mineralogy. Oxford University Press, New York, 495.

Nolan, P. J., Bone, S. E., Campbell, K. M., Pan, D., Healy, O. M., Stange, M., Bargar, J. R., Weber, K. A. 2021. Uranium (VI) attenuation in a carbonate-bearing oxic alluvial aquifer. Journal of Hazardous Materials 412, 125089.

Palmer, C. A., Tuncali, E., Dennen, K. O., Coburn, T. C., Finkelman, R. B. 2004. Characterization of Turkish coals: a nationwide perspective. International Journal of Coal Geology 60, 85–115.

Pedziwiatr, A., Potysz. A., Uzarowicz. L. 2021. Combustion wastes from thermal power stations and household stoves: A comparison of properties mineralogical and chemical composition and element mobilization by water and fertilizers. Waste Management 131, 136-146.

Perna, I., Supova, M., Hanzlicek, T. 2018. Gehlenite and anorthite formation from fluid fly ash. Journal of Molecular Structure 1157, 476-481.

Querol, X, Fernandez-Turiel, J. L, Lopez-Soler, A. 1995. Trace elements in coal and their behaviour during combustion in a large power station. Fuel 74, .331–43.

Querol, X., Whateley, M. K. G., Fernández-Turiel, J. L., Tuncali, E. 1997. Geological controls on the mineralogy and geochemistry of the Beypazari lignite, Central Anatolia, Turkey. International Journal of Coal Geology 33, 255–271.

Querol, X., Atastuey, A., Plana, F., Lopez-Soler, A., Tuncalı, E., Toprak, S., Ocakoğlu, F., Köker, A. 1999. Coal geology and coal quality of the Miocene Muğla basin, southwestern Anatolia Turkey. International Journal of Coal Geology 41, 311 –332.

Sarı, R., Küçükefe, Ş., Bozkaya, G., Bozkaya, Ö., Bademler, F., Aral, Z. D., Bayrakçıoğlu, E. D., Dönmez, C., Özkümüş, S. 2022. Geological, mineralogical-petrographical and fluid inclusion characteristics of the Çatalçam (Soma-Manisa) Au-Pb-Zn-Cu mineralization. Bulletin of the Mineral Research and Exploration 167, 25-49.

Seredin, V. V., Finkelman, R. B. 2008. Metalliferous coals: A review of the main genetic and geochemical types. International Journal of Coal Geology 70, 253–289.

Seredin, V. V., Danilcheva, Yu. A., Magazina, L. O., Sharova, I. G. 2006. Ge-Bearing Coals of the Luzanovka Graben, Pavlovka Brown Coal Deposit, Southern Primorye. Lithology and Mineral Resources 41, 280–301.

Shanmugam, G. 2024. Fossil fuels, climate change, and the vital role of CO2 plays in thriving people and plants on planet earth. Bulletin of the Mineral Research and Exploration 175, 167-208. https://doi.org/10.19111/bulletinofmre.1349959

Somay, M. A. 2017. Investigation of Güllük (Muğla) wetland by stable isotopes (d18O, dD). Bulletin of the Mineral Research and Exploration 154, 185-196.

Sütcü, E. 2021. Investigation of power plant coal ashes for economically important rare earth and trace elements. General Directorate of Mineral Research and Exploration Report No: 14019, 274, Ankara (unpublished).

Sütcü, E. C., Karayiğit, A. I. 2015. Mineral matter, majör and trace element content of the Afşin-Elbistan coals, Kahramanmaraş, Turkey. International Journal of Coal Geology 144-145, 111-129.

Sütcü, E. C., Şentürk, S., Kapıcı, K., Gökçe, N. 2021. Mineral and rare earth element distribution in the Tunçbilek coal seam, Kütahya, Turkey, International Journal of Coal Geology 245, 103820.

Taggart, R. K., Hower, J. C., Dwyer, G. S., Hsu-Kim, H. 2016. Trends in the rare earth element content of US–based coal combustion fly ashes. Environmental Science and Technology 50, 5919–5926.

Tamzok, N. 2017. Yerli kömüre dayalı termik santral potansiyeli, darboğazlar ve çözüm önerileri. Aytaç, O. (Ed.) Türkiye'de Termik Santraller, TMMOB Makine Mühendisleri Odası Yayını, 135-145.

Taş, A. 2009. Investigation of Origin at Barite Deposits in the Region of the Eastern Taurides (Adana-Feke). PhD Thesis, Çukurova University, 131, Adana (unpublished).

Tishmack, J. K., Olek, J., Diamond, S. 1999. Characterization of High-Calcium Fly Ashes and Their Potential Influence on Ettringite Formation in Cementitious Systems. Cement, Concrete, and Aggregates 21, 82–92.

TS-EN 197-1:2012. Standard Cement – Part 1: Composition, specification and conformity criteria for common cements. https://intweb.tse.org.tr.

Vassilev, S. V., Vassileva, C. G. 1996*a*. Occurrence. abundance and origin of minerals in coals and coal ashes. Fuel Processing Technology 8, 85–106.

Vassilev, S. V., Vassileva, C. G. 1996*b*. Mineralogy of combustion wastes from coal-fired power stations. Fuel Processing Technology 47, 261–280.

Vassilev, S. V., Vassileva, C. G. 2007. A new approach for the classification of coal fly ashes based on their origin, composition, properties, and behaviour. Fuel 86, 1490–1512.

Vassilev, S. V., Vassileva, C. G., Karayigit A. I., Bulut, Y., Alastuey, A., Querol, X. 2005. Phase-mineral and chemical composition of fractions separated from composite fly ashes at the Soma power station, Turkey. Environmental Science and Technology 61, 65–85.

Zielinski, R. A., Finkelman, R. B. 1997. Radioactive elements in coal and fly ash: abundance, forms, and environmental significance. U.S. Geological Survey, Fact Sheet FS 163-97.

Zhuang, X., Querol, X., Alastuey, A., Juan, R., Plana, F., Lopes-Soler, A., Du, G., Martynov, V. 2006. Geochemistry and mineralogy of the Cretaceous Wulantuga high germanium coal deposit in Shengli coal field, Inner Mongolia, Northeastern China. International Journal of Coal Geology 66, 119–136.